



# Review Article: Potential geomorphic consequences of a future great ( $M_w = 8.0+$ ) Alpine Fault earthquake, South Island, New Zealand

T. R. Robinson and T. R. H. Davies

Department of Geological Sciences, University of Canterbury, Private Bag 4800, Christchurch 8140, New Zealand

Correspondence to: T. R. Robinson (tom.robinson@pg.canterbury.ac.nz) and T. R. H. Davies (tim.davies@canterbury.ac.nz)

Received: 7 May 2012 – Published in Nat. Hazards Earth Syst. Sci. Discuss.: –

Revised: 4 June 2013 – Accepted: 17 June 2013 – Published: 23 September 2013

**Abstract.** The Alpine Fault in New Zealand's South Island has not sustained a large magnitude earthquake since ca. AD 1717. The time since this rupture is close to the average inferred recurrence interval of the fault ( $\sim 300$  yr). The Alpine Fault is therefore expected to generate a large magnitude earthquake in the near future. Previous ruptures of this fault are inferred to have generated  $M_w = 8.0$  or greater earthquakes and to have resulted in, amongst other geomorphic hazards, large-scale landslides and landslide dams throughout the Southern Alps. There is currently 85 % probability that the Alpine Fault will cause a  $M_w = 8.0+$  earthquake within the next 100 yr. While the seismic hazard is fairly well understood, that of the consequential geomorphic activity is less well studied, and these consequences are explored herein. They are expected to include landsliding, landslide damming, dam-break flooding, debris flows, river aggradation, liquefaction, and landslide-generated lake/fjord tsunamis. Using evidence from previous events within New Zealand as well as analogous international examples, we develop first-order estimates of the likely magnitude and possible locations of the geomorphic effects associated with earthquakes. Landsliding is expected to affect an area  $> 30\,000\text{ km}^2$  and involve  $> 1$  billion  $\text{m}^3$  of material. Some tens of landslide dams are expected to occur in narrow, steep-sided gorges in the affected region. Debris flows will be generated in the first long-duration rainfall after the earthquake and will continue to occur for several years as rainfall (re)mobilises landslide material. In total more than 1000 debris flows are likely to be generated at some time after the earthquake. Aggradation of up to 3 m will cover an area  $> 125\text{ km}^2$  and is likely to occur on many West Coast alluvial fans and floodplains. The impact of these effects will be felt across the entire South Island and is likely to continue for several decades.

## 1 Introduction

Great earthquakes have the potential to cause widespread and large-scale destruction not only in the built environment but also in the natural environment. Recent events, including the 2004 Sumatran earthquake, 2008 Wenchuan earthquake, and the 2011 Tohoku earthquake, have vividly demonstrated this. New Zealand is tectonically active with major fault systems distributed throughout the country. The North Island has several large, explosive volcanoes, an offshore subduction zone, and at least two major strike-slip faults. The South Island has offshore subduction zones to the north and south, a series of active strike-slip faults within the Marlborough system, and the Alpine Fault: a major strike-slip plate boundary fault that runs most of the length of the island (Fig. 1).

The Alpine Fault runs along the western range front of the Southern Alps (Figs. 1 and 2) and is a segment of one of the most active tectonic plate boundaries on earth. This fault has a 600 km long onshore surface expression. The well-defined 200 km long central segment accommodates most of the  $\sim 37\text{ mm a}^{-1}$  relative plate motion as a combination of dextral slip ( $\sim 70\%$ ) and uplift ( $\sim 30\%$ ). Recognised as a large-displacement source in the 1940s (Wellman and Willett, 1942) and generally accepted as a potential seismic source in the 1990s (Yetton, 1998), the Alpine Fault is now thought to be capable of generating great earthquakes ( $M_w \geq 8$ ) with a recurrence interval (average time between events) of the order of 200–400 yr (Berryman et al., 2012). The most recent rupture was ca. AD 1717, and involved a 380 km long segment of the fault (Yetton, 1998; Wells et al., 1999). Currently, there is an annual likelihood of rupture on the Alpine Fault of 1–2 % (Rhoades and Van Dissen, 2003). The Alpine Fault is chosen for this study as it is currently thought to be the most severe seismic hazard approaching or beyond its recurrence interval within New Zealand.

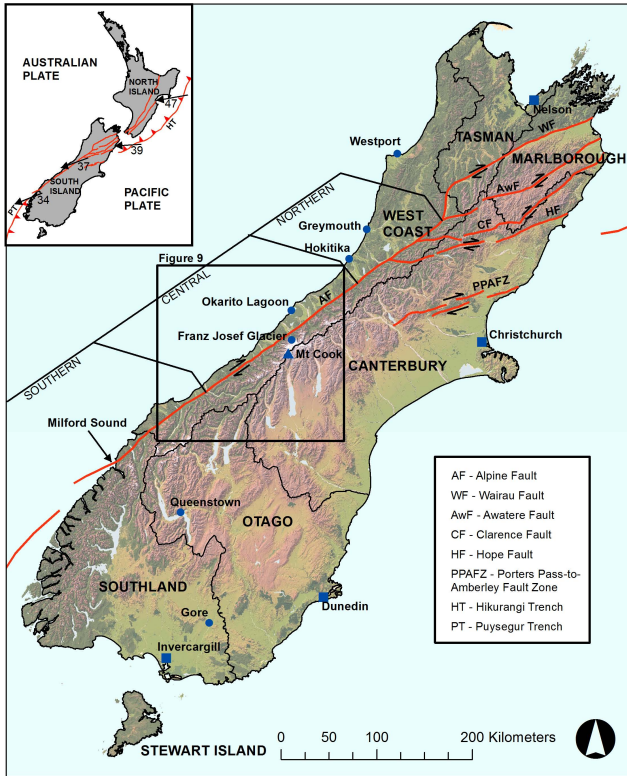


**Fig. 1.** Overview map of the South Island, New Zealand, showing the major fault systems. Inset: tectonic setting of New Zealand; arrows show plate vectors with velocities in  $\text{mm a}^{-1}$ .

The geomorphic consequences of an Alpine Fault earthquake and its aftershock sequence will change the South Island landscape and affect the environment for many years after the event. From observations of historical earthquakes worldwide, these impacts may include large landslides, landslide dams, dam-break floods, river aggradation and avulsion, lake tsunamis, ocean tsunamis, liquefaction, increased debris-flow activity, and glacier advance. Some of these effects are immediate, and some will be delayed onset; some will be short term and others long term; some will have local and others widespread impacts. Given that the South Island is only  $\sim 150$  km wide at its maximum, the next earthquake on the Alpine Fault has the potential to cause severe island-wide disruption.

The present work is an initial and necessary step in attempting to foresee the full range of geomorphic consequences associated with a great earthquake centred on the Alpine Fault. We first outline the likely seismic effects, then we describe the geomorphic effects with preliminary estimates of their spatial distribution and potential magnitudes. Much of this information is synthesised from a range of papers and reports published over the last several decades

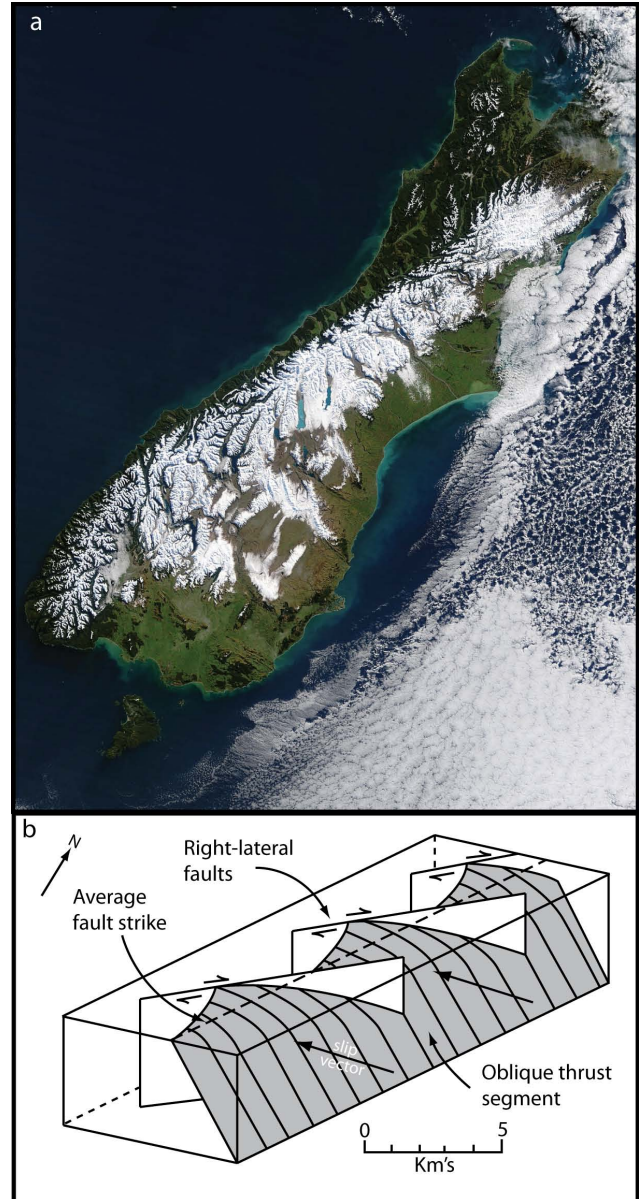


**Fig. 2.** (a) Satellite image of the South Island. The Alpine Fault can clearly be identified by the linear snow line on the Western edge of the Southern Alps; (b) simplified 3D model showing the complex segmentation of the Alpine Fault. Adapted from Norris and Cooper (1995).

investigating both historic and pre-historic earthquakes and their geomorphic consequences. We intend the present work to serve as a baseline compilation of likely processes, with order-of-magnitude estimates of their magnitudes and distributions, from which more detailed work can develop. We do not at this stage overlay facilities and infrastructure on the landscape effects in order to address societal risks.

## 2 Tectonic environment

### 2.1 Plate motion

The Alpine Fault marks the onshore boundary between the Australian and Pacific plates and accommodates the change from west-dipping subduction to the north (the Hikurangi Trench) to east-dipping subduction to the south (the Puysegur Trench) (Fig. 1). The rate of displacement across the plate boundary averaged over the last 3 million yr is  $37 \pm 2 \text{ mm a}^{-1}$  on a bearing of  $071 \pm 2^\circ$  (DeMets et al., 1994; Norris and Cooper, 2001). Along the central section of the fault this motion is partitioned  $35.5 \pm 1.5 \text{ mm a}^{-1}$  parallel and  $10 \pm 1.5 \text{ mm a}^{-1}$  perpendicular to the Alpine Fault resulting in a transpressional boundary (Norris and Cooper, 2001) with right-lateral-oblique motion. Strike-slip displacement rates along the central fault zone consistently average  $27 \pm 5 \text{ mm a}^{-1}$  while dip-slip rates vary widely with a maximum of  $> 12 \text{ mm a}^{-1}$  on the central segment (Norris and Cooper, 2001).

### 2.2 Fault systems

#### 2.2.1 Alpine Fault system

At a broad scale, the Alpine Fault appears as a simple linear feature striking SW–NE; however, in detail the fault is more complex (Fig. 2). The central segment of the fault is segmented at a scale of kilometres, consisting of north-striking oblique-reverse sections and east-striking dextral strike-slip sections (Fig. 2) (Norris and Cooper, 1995). The southern segment appears to simplify to a linear structure with little to no reverse motion (Berryman et al., 1992; Sutherland and Norris, 1995). Seismic reflection imaging in the Mt Cook region suggests that the fault dips  $\sim 40 \pm 5^\circ$  SE and continues to depths of  $\sim 25 \text{ km}$  (Davey et al., 1995).

Uplift of the Southern Alps as a result of plate motion is estimated to have begun between 10 Ma (Cooper, 1980; Kamp and Tippett, 1993) and 7 Ma (Kamp et al., 1989) with total uplift estimates of between 21.5 km (Kamp et al., 1989) and 25 km (Cooper, 1980). Total lateral offset along the fault is estimated at 480 km (Wellman, 1955; Berryman et al., 1992). This displacement is predominantly coseismic as little to no aseismic slip has been detected on the central and northern sections of the Alpine Fault (Beavan et al., 1999). Individual earthquake ruptures are estimated to result in 8–9 m dextral displacement with 2–3 m vertical displacement suggesting magnitudes of  $M_w \sim 8$  (Adams, 1980b; Hull and Berryman, 1986; Cooper and Norris, 1990; Sutherland and Norris, 1995; Sutherland et al., 2007). Rockfall deposits and other off-fault evidence similarly suggest that such events have  $M_w \sim 8$  (Adams, 1980b; Sutherland, 1994; Beavan et al., 1999; Leitner et al., 2001), though recent work indicates a slightly higher magnitude may be possible (De Pascale and Langridge, 2012).

Several instances of rupture on the Alpine Fault in the last ca. 1000 yr have been identified from fault trenching, tree coring of alluvial fan vegetation, studies of coastal dune ridges, and terrace displacements of West Coast rivers (Wells et al., 1999; Wells and Goff, 2007; Berryman et al., 2012; De Pascale and Langridge, 2012). These events have been dated to ca. AD 1717, ca. AD 1630, ca. AD 1460 and ca. AD 1230 (Fig. 3) suggesting a recurrence interval of  $\sim 200$ – $300 \text{ yr}$  (Sutherland, 1994; Wells et al., 1999; Leitner et al., 2001; Berryman et al., 2012).

#### 2.2.2 Other major fault systems

The Marlborough Fault System is the northern continuation of the Alpine Fault and consists of four major oblique dextral strike-slip faults (Bourne et al., 1998): the Wairau, Awatere, Clarence and Hope faults (Fig. 1). The northern faults of the Marlborough Fault System predominantly transfer plate motion to the onshore North Island dextral shear belt while the southern faults transfer stress to the Hikurangi subduction margin (Coulter, 2007). Rates of displacement since the late Quaternary have progressively increased to the south currently making the Hope Fault the most active segment of the Marlborough Fault System with slip rates of  $20$ – $25 \text{ mm a}^{-1}$  (Cowan, 1990; Cowan and McGlone, 1991; Van Dissen and Yeats, 1991; Langridge et al., 2003). This suggests that since the Hope Fault became the dominant branch of the Marlborough Fault System, the majority of accumulated strain has been released coseismically by this fault (Coulter, 2007).

South of the Marlborough Fault System a juvenile fault zone is forming on the edge of the plate boundary: the Porters Pass–Amberley Fault Zone (Fig. 1) (Cowan, 1992; Howard et al., 2003; Coulter, 2007). This is a complex zone of anastomosing faults and folds that includes the Porter's Pass, Ashley and Mt Grey Faults (Cowan, 1992). Historically no fault within the Porters Pass–Amberley Fault Zone has ruptured (Howard et al., 2003); nonetheless, the prominence of the surface trace of the Porter's Pass Fault suggests that repeated large-magnitude earthquakes have occurred on the fault over the last 10 000 yr (Howard et al., 2003). Total right-lateral, strike-slip offset along the Porters Pass–Amberley Fault Zone is estimated at 3 km since initiation of motion in the Holocene (Cowan, 1992).

### 2.3 Historical earthquakes

Since European settlement, only 2 earthquakes have been attributed to these major fault systems. These are the 1848 Blenheim earthquake, which occurred on the Awatere Fault and is estimated to have been  $M_w = 7.4$ – $7.5$  (Grapes et al., 1998), and the 1888 North Canterbury earthquake that occurred on the Hope Fault and had magnitude 7.0–7.3. In fact the majority of significant, historic onshore South Island earthquakes have not occurred on the major fault systems discussed above, but instead on more minor faults. Table 1

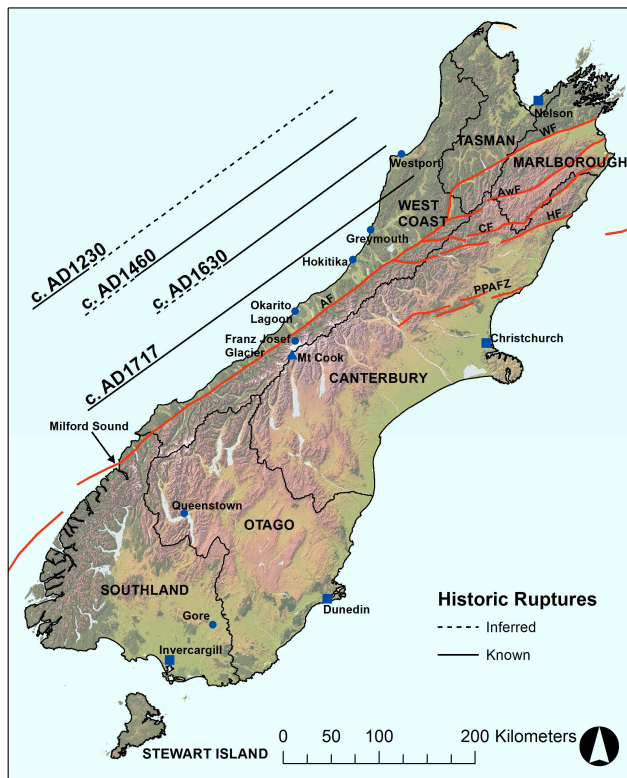


**Fig. 3.** Known and inferred rupture lengths of the last four Alpine Fault earthquakes.

lists the most significant earthquakes to have occurred in the South Island since European settlement.

Detailed information on the geomorphic impacts from these earthquakes only exists for the events after the 1968 Inangahua earthquake. The majority of these however, are subduction zone earthquakes and therefore may not be relevant to the Alpine Fault. Nevertheless, of the comparable earthquakes in the list the majority are known to have caused landsliding to some degree, while liquefaction and surface rupture were other common impacts (Table 1). The Buller and Inangahua earthquakes are known to have generated significant landsliding which resulted in numerous landslide dams (Adams, 1981). Given that such impacts have occurred historically throughout the Southern Alps as a result of earthquakes, it is anticipated that an Alpine Fault earthquake will cause many, if not all of the geomorphic effects listed in Table 1.

### 3 Physiography and geomorphology

The Southern Alps lie on the hanging wall of the Alpine Fault and formed as a result of the Australian-Pacific plate collision. They have an average elevation of  $\sim 1000\text{--}1500$  m with a maximum elevation of 3754 m at Mt Cook. The Southern Alps consist of Mesozoic greywacke and schist which alters

to mylonite, ultramylonite and cataclasite close to the Alpine Fault.

East of the Southern Alps, in the central-eastern South Island, lie the Canterbury Plains (Fig. 1). These consist of low-gradient alluvial fans, crossed by large, braided gravel-bed rivers (Gage, 1969). Parts of this region are at risk from river aggradation and avulsion even in the absence of an earthquake, while coastal estuarine sands and silts may be at risk of liquefaction from long-duration, distant source (i.e. low-frequency) shaking.

To the south the Canterbury Plains blend into older schist terrain with wide rolling hills (Fig. 1). In this region the effects from an Alpine Fault earthquake will be minor due to distance from the fault, with small-scale landsliding the most likely hazard; however, secondary fault activation due to stress transfer must also be considered. Again, the behaviour of major rivers is likely to be affected by landsliding upstream within the Southern Alps.

Rainfall across the South Island varies from a minimum of  $< 1000$  mm  $\text{a}^{-1}$  east of the Southern Alps to a maximum of  $> 11\,000$  mm  $\text{a}^{-1}$  in the western Southern Alps (Hicks et al., 1996). It is evenly distributed throughout the year with only minor differences between summer and winter rainfalls (Chinn, 2001).

Uplift rates for the Southern Alps indicate that  $\sim 600 \pm 100 \times 10^9$  kg of crustal rock are raised above sea level each year (Wellman, 1979; Adams, 1980a; Beaven et al., 2010b), and this is regionally close to total denudation (Griffiths, 1979; Adams, 1980a; Hovius et al., 1997). This results in South Island rivers carrying large sediment loads. Following an Alpine Fault earthquake, increases in river bedload sediment loads due to landsliding are likely to result in widespread river aggradation. Bedload sediment loads are difficult to quantify with estimates ranging from 10 % (Griffiths, 1979) to 50 % (Davies and McSaveney, 2006) of the total load. Therefore in the wake of an Alpine Fault earthquake it will be necessary to estimate the amount of additional available sediment in order to estimate the likely scale of river aggradation.

### 4 Physical processes

Following a large earthquake, widespread geomorphic consequences occur throughout the affected region on timescales varying from days to decades (Hewitt et al., 2008). The geomorphic consequences are intricately interlinked and have their own associated sets of hazards (e.g. Hewitt et al., 2008); Fig. 4 highlights the likely consequential hazards resulting from an Alpine Fault earthquake and the linkages between them. Some of these hazards will be short lived and others more prolonged, while some will have long-term effects possibly lasting for decades or more. Each of these hazards and their effects are described in more detail below.

**Table 1.** Significant earthquakes and their geomorphic effects for the South Island region, New Zealand, since European colonisation.

Year	Location	Region	Causative fault	Magnitude	Known geomorphic effects	Relevant references
1848	Blenheim	Marlborough	Awatere Fault	7.4–7.5	Surface rupture; landsliding	Grapes et al. (1998)
1855 <sup>a</sup>	Wairarapa	Wellington	Wairarapa Fault	8.0–8.2	Surface rupture; landsliding; landslide dam; dam-break flood; liquefaction; tsunami; seiche	Grapes and Downes (1997), Downes (2005), Hancox (2005)
1868 <sup>b</sup>	Farewell Spit	Tasman	Wakaramara Fault	7.2–7.6	Surface rupture	Anderson et al. (1994)
1869	Christchurch	Canterbury	Unknown	~ 6	Unknown	Pettinga et al. (2001)
1870	Christchurch	Canterbury	Unknown	5.5–6.0	Rockfall	Pettinga et al. (2001)
1881	Castle Hill	Canterbury	Castle Hill Fault?	6.0–6.8	Liquefaction	Pettinga et al. (2001)
1888	Lewis Pass	Canterbury	Hope Fault	7.0–7.3	Surface rupture	Smith and Berryman (1986), Cowan (1991)
1901	Cheviot	Canterbury	Unknown	6.9	Liquefaction; landsliding	Berril et al. (1994)
1922	Motunau	Canterbury	Unkown	6.4	Liquefaction; landsliding	Pettinga et al. (2001), Bull (2003)
1929	Arthurs Pass	Canterbury	Poulter Fault	7.0–7.1	Surface rupture; landsliding; landslide dams	Berryman and Villamor (2004)
1929	Buller (Murchison)	West Coast	White Creek Fault	7.3	Surface rupture; landsliding; landslide dams	Dowrick (1994)
1968	Inangahua	West Coast	Inangahua Fault? Lyell Fault?	7.1	Landsliding; landslide dams	Adams (1981), Anderson et al. (1994)
1988 <sup>c</sup>	Te Anau	Southland	Puysegur trench	6.7	Landsliding	Reyners et al. (1991)
1993 <sup>c</sup>	Secretary Island	Southland	Puysegur trench	6.8	Landsliding; tsunami	Reyners and Webb (2002)
1994	Arthurs Pass	Canterbury	Unknown	6.7	Landsliding; avalanches (snow)	Robinson et al. (1995)
2003 <sup>c</sup>	Fiordland	Southland	Puysegur trench	7.2	Landsliding; tsunami	Power et al. (2005)
2007 <sup>c</sup>	George Sound	Southland	Puysegur trench	6.7	Landsliding	Peterson et al. (2009)
2009 <sup>c</sup>	Dusky Sound	Southland	Puysegur trench	7.8	Landsliding	Beavan et al. (2010a)
2010	Darfield	Canterbury	Greendale Fault	7.1	Surface rupture; liquefaction	Quigley et al. (2010), Gledhill et al. (2011)
2011	Christchurch	Canterbury	Lyttelton Fault	6.3	Liquefaction; rockfall	Beavan et al. (2011), Holden (2011)

<sup>a</sup> Epicentre in the North Island, but severe shaking generated in the northern South Island, <sup>b</sup> epicentre offshore but noticeable surface rupture onshore, and <sup>c</sup> offshore subduction zone earthquakes.

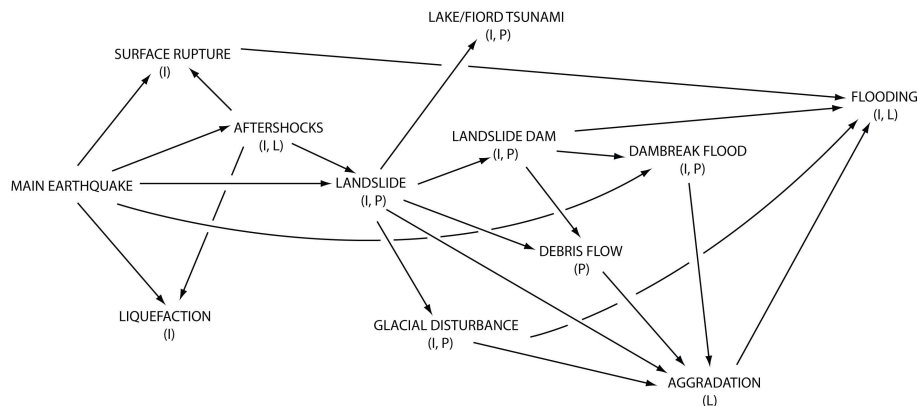


**Fig. 4.** Flow chart of geomorphic consequences resulting from an earthquake. I – immediate: occurring seconds to days after the event; P – prolonged: lasting weeks to years; L – long-term: lasting years to decades.

#### 4.1 The great earthquake

Present estimates of fault locking depth are  $\sim 10$  km (Beavan et al., 1999) or deeper (Beavan et al., 2010b) for each section of the fault. This suggests that the next Alpine Fault earthquake is likely to occur at a relatively shallow depth of 8–12 km. Studies by Bull (1996), Yetton (1998), Wells et al. (1999), and Wells and Goff (2007) (Fig. 3) show that the northern and central sections of the Alpine Fault usually rupture during great earthquakes while the southern section may be less frequently activated.

Accurately predicting the exact epicentre location is difficult with current scientific understanding; however, we identify a most likely region for the epicentre to occur. We suggest that given the last known Alpine Fault earthquake appears to have involved the full length of the fault (Fig. 3), the highest strain has since accumulated in the region with the largest slip rate. According to Norris and Cooper (2001), the largest slip occurs in the Mt Cook region and we therefore suggest that this area is the most likely region for epicentre to occur.

From previous rupture lengths (Fig. 3), we suggest that rupture will most likely involve the northern and central sections and possibly the southern section as well (Fig. 5). Surface ruptures with  $\sim 8$  m lateral and  $\sim 1$ –2 m vertical displacement (Berryman et al., 2012) are possible along the entire rupture length. In the immediate vicinity of the epicentre ground shaking is likely to reach Modified Mercalli Intensity (MM) X or higher (N. Pondard, personal communication, 2012) (see Table 2). Local conditions along the fault may result in MM XI or XII and the entire South Island may experience MM > V (Fig. 5).

The duration of shaking is closely related to the duration of fault rupture which depends on rupture length and rupture speed. During the 1906  $M_w = 7.8$  San Francisco earthquake rupture speed was estimated to have averaged  $\sim 3.2$  km s<sup>-1</sup> and peaked at  $\sim 3.7$  km s<sup>-1</sup> (USGS, 2012). This earthquake has similar seismic properties to our suggested Alpine Fault earthquake in that it

1. occurred on a right-lateral oblique slipping fault (northern San Andreas Fault);
2. had rupture length of  $\sim 400$  km;
3. had an epicentre in the centre of the rupture section resulting in bidirectional rupture;
4. had lateral slip of up to 9.2 m; and
5. was  $M_w = 7.8$  (USGS, 2012).

Should the rupture speed of an Alpine Fault earthquake be similar to that of the San Francisco earthquake ( $\sim 3.2$  km s<sup>-1</sup>), rupture of the entire Alpine Fault ( $\sim 450$  km from end to end, or  $\sim 225$  km from a central epicentre) could last 70 s. However, should the epicentre not occur in the middle of the fault but at either end, the shaking duration would

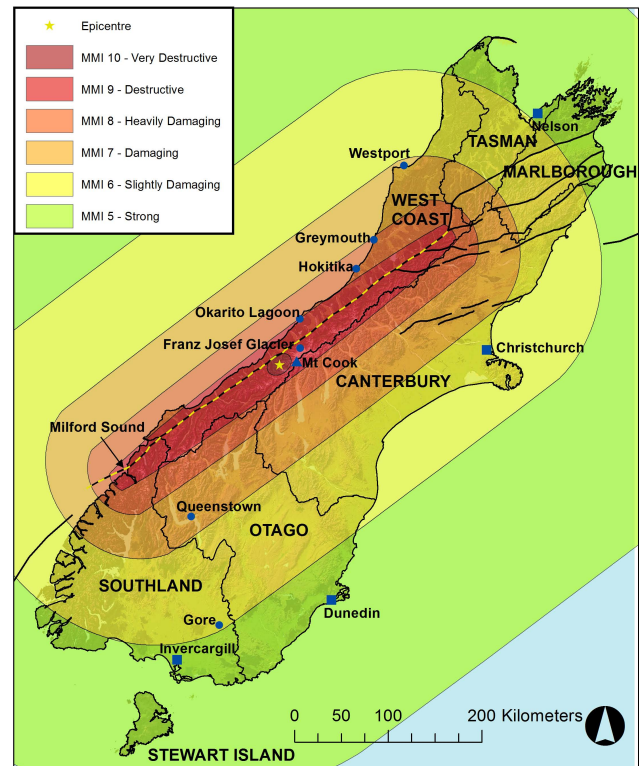


**Fig. 5.** Isoseismal model for a  $M_w = 8.0$  earthquake occurring on the central segment of the Alpine Fault. Based on the isoseismal models of Smith (1978), produced by N. Pondard of GNS Science at the authors request. Black and Yellow dashed line shows expected rupture length.

double to around 140 s. In 2001 a  $M_w = 7.8$  earthquake occurred on the left-lateral Kunlun Fault in the Tibet region resulting in a  $\sim 400$  km long rupture with lateral displacements of 7–8 m (Bouchon and Vallée, 2003; Robinson et al., 2006). This event appears to have had highly variable rupture speeds ranging from 2.4 km s<sup>-1</sup> to 5 km s<sup>-1</sup> at various points along the rupture (Bouchon and Vallée, 2003; Robinson et al., 2006). It is not improbable that such variability may be seen in an Alpine Fault earthquake and as such we incorporate this into our estimate of rupture duration suggesting that it may last  $70 \pm 20$  s for a central epicentre, and  $140 \pm 50$  s for a distal epicentre.

#### 4.2 Aftershock sequence

All aftershock sequences are unique, but it is possible to make general statements about the likely maximum magnitude, number, and decay pattern of aftershocks resulting from an Alpine Fault earthquake. Utsu (1970) showed that the difference,  $D_1$ , between the main event magnitude,  $M_m$ , and the maximum aftershock magnitude,  $M_{amax}$ , could be

**Table 2.** The Modified Mercalli Intensity scale (Wood and Neumann, 1931).

Intensity	Description	
I	Imperceptible	Barely sensed only by a very few people.
II	Scarcely felt	Felt only by a few people at rest in houses or on upper floors.
III	Weak	Felt indoors as a light vibration. Hanging objects may swing slightly.
IV	Largely observed	Generally noticed indoors, but not outside, as a moderate vibration or jolt. Light sleepers may be awakened.
V	Strong	Generally felt outside and by almost everyone indoors. Most sleepers are awakened and a few people alarmed.
VI	Slightly damaging	Felt by all. People and animals are alarmed, and many run outside. Walking steadily is difficult.
VII	Damaging	General alarm. People experience difficulty standing. Furniture and appliances are shifted.
VIII	Heavily damaging	Alarm may approach panic. A few buildings are damaged and some weak buildings are destroyed.
IX	Destructive	Some buildings are damaged and many weak buildings are destroyed.
X	Very destructive	Many buildings are damaged and most weak buildings are destroyed.
XI	Devastating	Most are damaged and many buildings are destroyed.
XII	Very devastating	All buildings are damaged and most buildings are destroyed.

determined by

$$D_1 \approx 5.0 - 0.5M_m \quad (\text{for } M_m > 6.0). \quad (1)$$

Therefore, for an Alpine Fault earthquake with  $M_m = 8.0$  the maximum aftershock magnitude is  $M_{\text{amax}} \approx 7.0$ . This agrees with Hainzl et al. (2000) who stated that the largest aftershock is typically one unit smaller than the main earthquake. Nonetheless, Utsu (1970) noted that previous estimates of  $D_1$  obtained from analysis of 90 Japanese earthquakes varied between 0 and 3. On this basis, for a  $M_w = 8.0$  Alpine Fault earthquake,  $M_{\text{amax}}$  could range from  $M_w = 5.0$ – $8.0$ .

Solov'ev and Solov'eva (1962) showed that the number of aftershocks,  $k$ , with magnitude  $M > M_m - 2.0$  fitted an exponential decay. They also established that the mean value of  $k$  decreases with focal depth such that

$$k = 160/h, \quad (2)$$

where  $h$  is the focal depth of the main earthquake in km. An earthquake on the Alpine Fault is likely to have a focal depth of between 8 and 12 km, suggesting there could be between 13 and 20 aftershocks with  $M > 6.0$ .

It may also be possible to determine the likely time,  $T_1$ , between  $M_m$  and  $M_{\text{amax}}$ . Utsu (1970) plotted data for all Japanese earthquakes ( $M > 5.5$ ) between 1959 and 1969 and their largest aftershock, and found a correlation between  $M_m$  and  $T_1$  such that

$$\log \bar{T}_1 \approx 0.5M_m - 3.5, \quad (3)$$

where  $\bar{T}_1$  is the mean time in days. For a  $M_w = 8.0$  earthquake this corresponds to a time of 3 days between the main earthquake and the largest aftershock. However, Utsu (1970) also noted that there was much scatter between  $T_1$  and  $M_m$  and that  $T_1$  varied between  $0.01\bar{T}_1$  and  $100\bar{T}_1$ . This suggests a likely range of 0.03 days ( $\sim 40$  min) to 300 days. We therefore suggest that  $M_{\text{amax}}$  is likely to occur at any time within a year of the main earthquake.

A more appropriate method for analysing the timing and decay of an aftershock sequence is the Modified Omori Formula as demonstrated in Utsu et al. (1995). This determines

the frequency of earthquakes,  $n(t)$ , per day, in terms of time,  $t$ , since the main earthquake:

$$n(t) = k(t + c)^{-p}, \quad (4)$$

where  $k$ ,  $c$ , and  $p$  are constants to be calculated. Utsu et al. (1995) showed that the values of  $c$  and  $p$  were dependent on the magnitude of aftershocks being considered and presented data for various sizes. Figure 6 shows the aftershock decay fitted by Utsu et al. (1995) using the Modified Omori Formula following the  $M = 7.8$  Nansei-Oki earthquake in 1993 for aftershocks with  $M > 3.2$  and  $M > 4.0$ . We present Fig. 6 as an example of the aftershock decay following a  $M_w \sim 8.0$  earthquake on the Alpine Fault. It indicates that 100 days after the main earthquake, aftershocks  $> M = 3.2$  are still occurring at  $\sim 3$  per day.

### 4.3 Landsliding

Landslides of all sizes are always a major hazard in the Southern Alps due to the steep topography combined with the high annual rainfall and seismicity on active faults. While not all landslides are seismically derived, the majority of rapid, large ( $> 10^6 \text{ m}^3$ ), deep-seated landslides result from high-intensity shaking (Whitehouse and Griffiths, 1983). Seismic shaking, however, will cause both shallow- and deep-seated landslides throughout the Southern Alps.

Maximum run-out distances for landslides are related to the total fall height by the formula:

$$L = H / \tan \alpha, \quad (5)$$

where  $H$  is total fall height in m,  $L$  is runout distance in m, and  $\tan \alpha$  is the coefficient of friction (Hsü, 1975).  $H$  is likely to be several hundred metres, while  $\tan \alpha$  is typically  $\sim 0.6$  which suggests runout distances in excess of  $\sim 1$  km; however, very large landslides ("sturzsstroms",  $> 10^6 \text{ m}^3$ ) may have much longer run-outs (Hsü, 1975). A rock avalanche containing  $\sim 45 \times 10^6 \text{ m}^3$  material from Round Top, West Coast region ran out for over 4 km with a total fall height

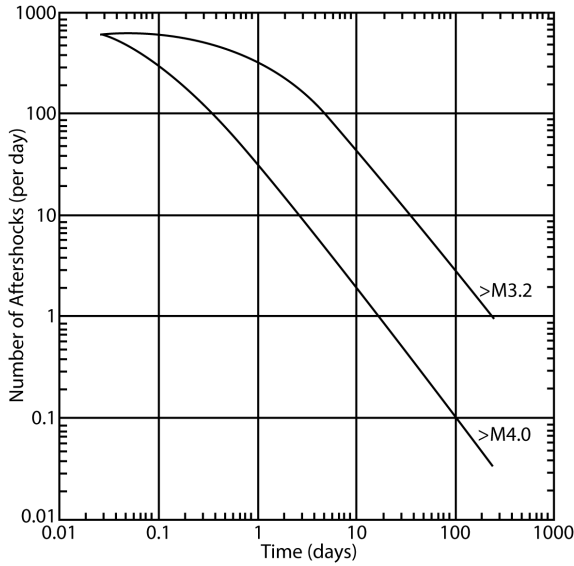


**Fig. 6.** Possible aftershock decay model following a  $M_w = 8.0$  earthquake. From Utsu et al. (1995).

of only  $\sim 500$  m (Wright, 1998). This landslide may have been seismically triggered, being deep seated and having occurred in ca. AD 930, around the same time as a major Alpine Fault earthquake (Wright, 1998). Other landslides identified by Yetton et al. (1998) as well as eight rock avalanches identified throughout the Southern Alps (Bull, 1996) are also thought to be associated with the same Alpine Fault event and further highlight the likely extent of landsliding that can be expected in future events.

Keefer (1984) and Malamud et al. (2004) have attempted to relate earthquake magnitude to landsliding. Using observational data from Keefer (1984) along with calculated data from the 1994 Northridge earthquake (Table 3), Malamud et al. (2004) obtained

$$\log N_{LT} = 1.27M - 5.45(\pm 0.46), \tag{6}$$

where  $N_{LT}$  is the total number of landslides generated, and  $M$  is the moment magnitude of the earthquake. While this formula and its associated error fit the available data, Table 3 demonstrates the different scales that can be produced from similar magnitude earthquakes. For instance, the  $M_w = 6.9$  Hygoken-Nanbu earthquake generated just 700 landslides while the  $M_w = 6.7$  Northridge earthquake generated 11 000. Using this formula to determine the number of landslides from a future earthquake is therefore useful for an order of magnitude estimate but demonstrates a large range in possible values (Table 4).

Keefer (1984) found that the area affected by coseismic landsliding,  $A$ , in  $\text{km}^2$ , correlated with earthquake magnitude, although focal depth, specific ground motion, and geologic conditions were also important. This was confirmed by

**Table 3.** Earthquake location, date and moment magnitude,  $M$ , with total landslide volume,  $V_{LT}$ , and total landslide numbers,  $N_{LT}$ , from Keefer (1984) including data from Northridge, CA (Malamud et al., 2004) and Wenchuan, China (various, see text).

Location	Date	$M$	$V_{LT}$ ( $\text{m}^3$ )	$N_{LT}$
Arthur's Pass, New Zealand	9 Mar 1929	6.9	$5.90 \times 10^7$	
Buller, New Zealand	17 Jun 1929	7.6	$1.30 \times 10^9$	
Torricelli Mtns, New Guinea	20 Sep 1935	7.9	$2.15 \times 10^8$	
Assam, India	15 Aug 1950	8.6	$4.70 \times 10^{10}$	
Daily City, CA, USA	22 Mar 1957	5.3 <sup>a</sup>	$6.70 \times 10^4$	23
Inangahua, New Zealand	23 May 1968	7.1	$5.20 \times 10^7$	
Peru	31 May 1970	7.9	$1.41 \times 10^8$	
Papua New Guinea	31 Oct 1970	7.1	$2.80 \times 10^7$	
Guatemala	11 Jul 1976	7.6	$1.16 \times 10^8$	50 000
Darien, Panama	4 Feb 1976	7.0	$1.30 \times 10^8$	
Mt Diablo, CA, USA	24 Jan 1980	5.8 <sup>b</sup>		103
Mammoth Lakes, CA, USA	25 May 1980	6.2	$1.20 \times 10^7$	5253
Coalinga, CA, USA	2 May 1983	6.5	$1.94 \times 10^6$	9389
San Salvador, El Salvador	10 Oct 1986	5.4	$3.78 \times 10^5$	216
Ecuador	5 Mar 1987	7.2	$9.53 \times 10^7$	
Loma Prieta, CA, USA	17 Oct 1989	7.0	$7.45 \times 10^7$	1500
Northridge, CA, USA	17 Jan 1994	6.7	$1.20 \times 10^8$ <sup>c</sup>	11 000
Hygoken-Nanbu, Japan	17 Jan 1995	6.9		700
Umbria-Marche, Italy	26 Sep 1997	6.0		110
Chi-Chi, Taiwan	21 Sep 1999	7.7		22 000
Wenchuan, China	12 May 2008	8.0	$1.5\text{--}15 \times 10^9$	$> 56\,000$

<sup>a</sup> Surface-wave magnitude,  $M_S$ . <sup>b</sup> Local magnitude,  $M_L$ . <sup>c</sup> Volume calculated from summation of individual landslide volumes.

**Table 4.** Summary of landslide variables calculated from formulae by Keefer and Wilson (1989) and Malamud et al. (2004) following a  $M_w = 8.0$  earthquake on the Alpine Fault.

	Minimum	Mean	Maximum
<sup>a</sup> Total number of landslides, $N_{LT}$	17 782	51 286	147 910
<sup>b</sup> Total affected area, $A$ ( $\text{km}^2$ )	11 749	34 673	102 329
<sup>a</sup> Total landslide area, $A_{LT}$ ( $\text{km}^2$ )	55	158	457
<sup>a</sup> Largest landslide area, $A_{Lmax}$ ( $\text{km}^2$ )	1.3	2.7	5.8
<sup>a</sup> Total landslide volume, $V_{LT}$ ( $\text{km}^3$ )	0.4	1.3	4.2
<sup>a</sup> Largest landslide volume, $V_{Lmax}$ ( $\text{km}^3$ )	0.07	0.2	0.6

<sup>a</sup> Determined from Malamud et al. (2004); <sup>b</sup> determined from Keefer and Wilson (1989).

Keefer and Wilson (1989) who showed that

$$\log A = M - 3.46(\pm 0.47)(5.5 < M \leq 9.2). \tag{7}$$

Applied to the South Island, this suggests that following a  $M_w = 8.0$  Alpine Fault earthquake landslides are likely to occur across an area of  $\sim 35\,000$   $\text{km}^2$  (Table 4).

Malamud et al. (2004) also related  $M$  to total landslide area,  $A_{LT}$  ( $\text{km}^2$ ), total landslide volume,  $V_{LT}$  ( $\text{km}^3$ ), largest landslide area,  $A_{Lmax}$  ( $\text{km}^2$ ), and largest landslide volume,  $V_{Lmax}$  ( $\text{km}^3$ ):

$$\log A_{LT} = 1.27M - 7.96(\pm 0.46), \tag{8}$$

$$\log V_{LT} = 1.42M - 11.26(\pm 0.52), \tag{9}$$

$$\log A_{Lmax} = 0.91M - 6.85(\pm 0.33), \tag{10}$$

$$\log V_{Lmax} = 1.36M - 11.58(\pm 0.49). \tag{11}$$

These formula are again useful for an order of magnitude estimate; however, Table 3 shows the variability that exists for similar sized earthquakes. For instance the  $M_w = 7.6$  Buller earthquake generated  $1.3 \times 10^9 \text{ m}^3$  of sediment while the larger  $M_w = 7.9$  Torricelli Mountains earthquake generated just  $2.15 \times 10^8 \text{ m}^3$ . This is probably an effect of local conditions with the Buller earthquake occurring in steep, formerly glaciated terrain and therefore being particularly susceptible to landsliding. Furthermore, these formula cannot anticipate extreme events such as the Daguangbao landslide generated by the 2008  $M_w = 8.0$  Wenchuan earthquake. Huang et al. (2011) stated that this landslide had an area of  $7.8 \text{ km}^2$ ,  $\sim 2 \text{ km}^2$  more than the maximum Eq. (10) suggests. Similarly, Huang et al. (2011) stated a volume of  $0.75 \text{ km}^3$  for this landslide,  $0.13 \text{ km}^3$  more than the maximum Eq. (11) suggests. These formula are therefore effective for showing a typical range of likely magnitudes, but are not able to identify the occurrence of extreme events.

Table 4 shows the results of the above relationships for a  $M_w = 8.0$  earthquake. Minimum and maximum do not refer to the extreme values limited by the laws of physics but merely the largest and smallest values that could occur and would still fit the empirical formulae; both smaller and larger events such as the Daguangbao landslide are possible but inherently unlikely.

From this we suggest that following an Alpine Fault earthquake, landsliding of all scales is likely to occur along the entire rupture length with the greatest damage in the highest-intensity shaking zones (see Fig. 5). Aftershocks on subordinate fault systems may extend the area affected by landsliding to the extent that much of the mountainous area of the South Island may be at risk. For example, an aftershock in the Marlborough Fault System would be likely to cause landsliding in the Kaikoura Ranges, which are unlikely to be affected by an Alpine Fault earthquake. While not all regions will suffer from large landslides, it is expected that smaller, shallow-seated landslides will occur widely in hilly country, especially following subsequent rainfall. Further landsliding is likely to occur for several years throughout the South Island during aftershocks and rainstorms. Landslides will also affect water bodies, as we discuss next.

#### 4.4 Landslide dams

Large landslides falling into and blocking rivers form landslide dams and landslide dammed lakes. These have a number of associated up- and downstream hazards, but the most significant hazards result from the failure of the dam generating both an immediate dam-break flood and subsequent, longer-term river aggradation as the landslide material is re-worked downstream.

At least 232 landslide dams have been recorded in New Zealand in recent history (Korup, 2004, 2005), including 140 currently with landslide dammed lakes (Korup, 2004). New Zealand has some of the largest landslide dammed lakes in

the world, for example the largest, in the central North Island, has a total water volume of  $5 \times 10^9 \text{ m}^3$  (Davies et al., 2005). Data on frequency of dam failure and age of surviving dams are currently inadequate; however, dams that have been dated appear to cluster to specific dates, suggesting a shared cause like an earthquake (Korup, 2005). Costa and Schuster (1988) estimate that up to 90 % of landslide dams are the result of seismic shaking or intense rainfall events.

The key attribute required for assessment of landslide dam hazards is the stability of the dam against rapid failure. Experience, however, shows that the stability of a landslide dam is purely a statistical concept (Nash et al., 2008), and in outlining hazards consequential on an Alpine Fault earthquake, all landslide dams that form can be considered as potential sources of dam-break floods and aggradation.

McCahon et al. (2006a) identified 15 river catchments in the Southern Alps that were likely to be blocked by landslides generated by an Alpine Fault earthquake (Fig. 7). These each have steep sides and narrow valleys, which are required for the formation of a landslide dam. These catchments include the Poerua River where a landslide dam formed and failed in 1999 (see below) and the Callery gorge, which has also been identified by Davies and Scott (1997) as a potential location. Furthermore, these include the Maruia and Matakita rivers, where landslide dams previously formed in the 1929 Buller earthquake (Adams, 1981). The Buller river has also been shown by Adams (1981) to be regularly blocked by landsliding, and landslide dams formed here during the 1929 Buller and 1968 Inangahua earthquakes (Table 1). Landslides during the Buller earthquake are also known to have blocked the Karamea and Mokihinui rivers (Adams, 1981).

As shown by Adams (1981) there are many more catchments susceptible to landslide damming than those identified by McCahon et al. (2006a). The Waimakariri gorge east of the main divide is one such example. A dam here presents a significant hazard to the downstream developments including the city of Christchurch. Following the 2008 Wenchuan earthquake  $> 30$  landslide dams (Li et al., 2012) formed across a landslide affected area of  $> 20000 \text{ km}^2$  (Gorum et al., 2011). Given the large number of catchments with suitable characteristics for landslide dam formation, an anticipated landslide-affected area similar to Wenchuan (Table 4), and that multiple landslide dams have been known to form in historic South Island earthquakes, we suggest some tens of landslide dams could form following an Alpine Fault earthquake. It is likely that some or all of the catchments identified by McCahon et al. (2006b) as well as the Buller, Karamea, and Mokihinui rivers will be blocked (Fig. 7). A blockage in the Waimakariri gorge is also possible. We discuss the hazard resulting from failure of these dams in the following section.

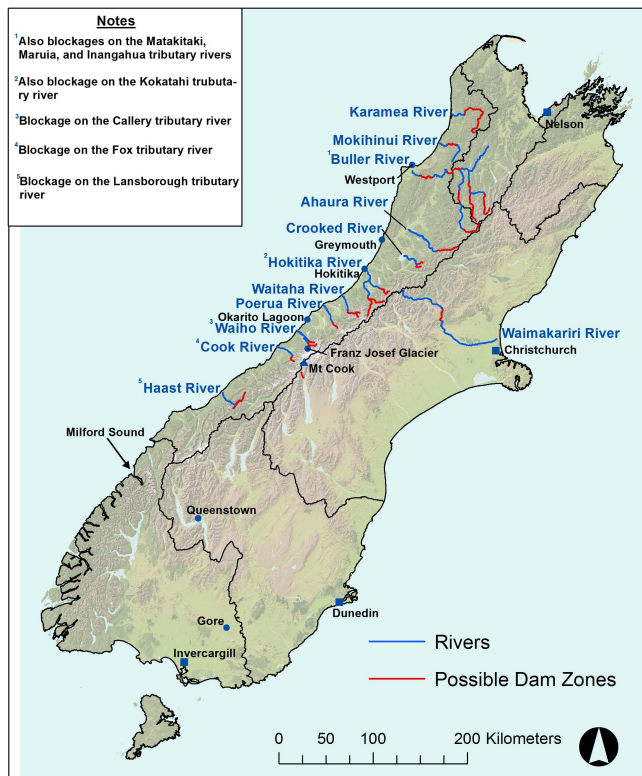


Fig. 7. South Island rivers susceptible to landslide dam formation.

#### 4.5 Dam-break floods

Outburst floods or dam-break floods are the most obvious hazard resulting from landslide dams. They occur as the result of full or partial dam failure releasing the impounded water to cause major, rapid-onset flooding downstream, with the dam sediment causing substantial aggradation both during the failure and subsequently. Dam failure results from overtopping, seismic shaking, heavy rain or a combination of each (Korup, 2005). Costa and Schuster (1988) found that 27 % of dams fail within 1 day of formation while only 15 % survive for more than 1 year. Nonetheless, statistically only 35 % of known New Zealand dams have failed; however, Korup (2005) and Korup and Tweed (2007) note that this is most likely an artefact of under-reporting and under-sampling of dam formation and recognition of failed dams due to the often remote location of such events.

In 2007 a large landslide dam formed in the Young River in the South Island, and was identified by chance by a helicopter pilot flying over the area. Analysis of seismic records showed that this event had occurred 3 weeks before it was discovered (GNS Science, 2012). This was primarily due to the remote location of the landslide and the lack of downstream river level gauges. As of 2013 this dam and the resultant lake are still intact and thus present a continued downstream hazard. Long-term hazard from these dams is further indicated by the fact that Costa and Schuster (1991) reported some in-

stances of dam failure *centuries* after the initial blockage formed. Following an Alpine Fault earthquake some dams may survive indefinitely. This will cause a continued, long-term downstream hazard. Nevertheless, dams existing at the initiation of shaking of an Alpine Fault earthquake are at risk of failure either directly from shaking or as a result of a landslide generated wave overtopping the dam. The Young River landslide dam is < 25 km from the Alpine Fault and is likely to receive shaking intensities of MM IX or greater. Further landsliding in the vicinity may impact the lake generating an overtopping wave which would likely result in the collapse of the dam.

The best-studied example of landslide dam-break flooding within New Zealand is that from the 1999 Mt Adams rock avalanche, which blocked the Poerua River. The landslide, which had a volume of  $10\text{--}15 \times 10^6 \text{ m}^3$ , blocked the river to a depth of  $\sim 120 \text{ m}$  and formed a lake with volume  $5\text{--}7 \times 10^6 \text{ m}^3$  (Hancox et al., 2005; Becker et al., 2007). This lake formed and the dam overtopped within 48 h, however it did not immediately fail (Becker et al., 2007), remaining intact for 5 days until overnight rainfall on the 6th night resulted in the dam breaching (Hancox et al., 2005). In the Poerua gorge immediately downstream of the dam the flood peak is inferred to have reached  $\sim 5 \text{ m}$  in height and travelled at up to  $5 \text{ ms}^{-1}$  (Davies, 2002; Hancox et al., 2005). The flood in the Poerua valley peaked at  $\sim 2 \text{ m}$  above normal flow levels (Davies, 2002; Hancox et al., 2005; Becker et al., 2007). The dam-break resulted in  $\sim 75 \%$  of the lake being drained causing a short-duration peak flow of  $\sim 3000 \text{ m}^3 \text{ s}^{-1}$  (Davies, 2002; Hancox et al., 2005; Davies et al., 2007). In the years following the breach, severe damage has been caused by dam sediment being reworked downstream by the river and aggrading the valley floor substantially and extensively.

The formation and eventual failure of landslide dams throughout the Southern Alps will be a continued and prolonged consequence of an Alpine Fault earthquake due to aftershocks. The area likely to be affected by such failures is far larger than the immediate area affected by the landslide and lake, and communities many kilometres from large dams may be at high risk. Following the 2008 Wenchuan earthquake, > 30 landslide dams formed, some threatening communities up to 30 km away (Li et al., 2012).

#### 4.6 Aggradation

Davies and Korup (2007) trenched alluvial fans in the West Coast region in order to establish when they were last active and thus determine the last time they aggraded. Within the Poerua fan they identified at least 2 paleo-soils. On the Tartare fan 2 paleo-soils were found between massive gravels whose age was hundreds of years. No buried soils were found in the Waiho fan, but a massive medium sand layer identified at  $\sim 5 \text{ m}$  depth dated to between 1616 and 1682. Similar stratigraphy was found at Fox River. Davies and

Korup (2007) inferred that this evidence represented aggradation that occurred on each of these fans after the ca. 1615 Alpine Fault earthquake. Similar results were found in the Whataroa fan where current soils date back only to  $\sim 1620$  (Berryman et al., 2001). It is therefore likely that most West Coast alluvial fans have witnessed large-scale aggradation following some Alpine Fault earthquakes.

Following the 1999 Poerua dam-break flood it is estimated that within 6 yr  $1.0\text{--}1.5 \times 10^6 \text{ m}^3$  of sediment was (re)mobilised and deposited on the Poerua alluvial fan which extends for  $\sim 5 \text{ km}$  (Davies et al., 2005). Hancox et al. (2005) noted that by 2003 alluvium deposited in the Poerua River channel had raised a tributary to 25 m above its 1992 level. This has resulted in widespread gravel deposition through rainforest-covered terraces, destroying much of the vegetation. Aggradation of  $> 10 \text{ m}$  elevated the river bed so that the river flowed across the fan surface into which it was previously incised, resulting in severe damage (Davies et al., 2005; Hancox et al., 2005). By 2001 aggradation had caused the flow of the river to shift  $\sim 800 \text{ m}$  east, actively eroding a channel across farmland and another tributary's alluvial fan (Fig. 8) (Hancox et al., 2005). This event is estimated to have added the equivalent of 500 years of normal supply of sediment to the fan head in just 6 yr (Davies et al., 2005) and the effects are expected to last for decades as sediment currently remaining in the dam and gorge is gradually and continually reworked (Hancox et al., 2005). The aggradation at the fan head appeared to peak about decade after the landslide.

Following an Alpine Fault earthquake and widespread landsliding, sediment carried by rivers as suspended load will be largely transported offshore. Much of the accompanying bedload, however, will be deposited within river channels and on alluvial fans and floodplains causing aggradation. Much of this deposition will be long-term because re-incision of the river following peak aggradation will only very slowly rework the deposited bedload. Given the total volume of sediment likely to be available after an Alpine Fault earthquake from Table 4, and estimates of the proportion of bedload to total sediment load (from 10 %, Griffiths, 1979, to 50 %, Davies and McSaveney, 2006), it is possible to estimate the area likely to be affected by a specific depth of aggradation. We anticipate aggradation will be on the order of metres and therefore calculate the area likely to be affected by aggradation of 3 m from

$$\text{Area affected} = \frac{\text{Volume of sediment available}}{\text{Aggradation}}. \quad (12)$$

This assumes that none of the bedload reaches the sea which is only true in the short-term. All of the bedload is temporarily deposited on fans and floodplains before slowly being reworked and transported offshore. Using the mean value of  $V_{LT}$  (Table 4) of  $1.3 \times 10^9 \text{ m}^3$ , and assuming that bedload yields account for 30 % (from the estimates of Griffiths, 1979 and Davies and McSaveney, 2006), aggradation of 3 m will affect an area of  $125 \times 10^6 \text{ m}^2$  ( $125 \text{ km}^2$ ). Using the extreme

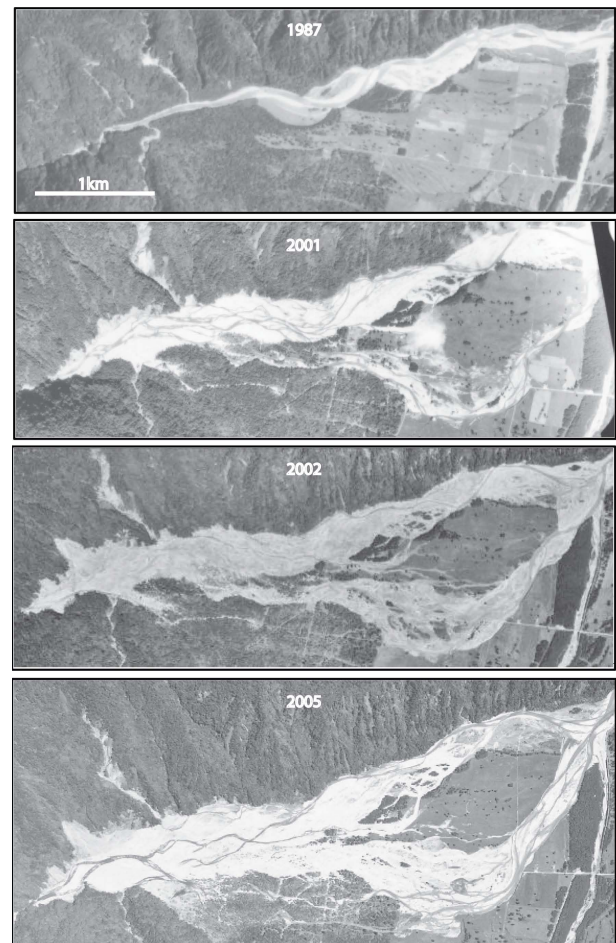


**Fig. 8.** Aerial photos of the Poerua River from 1987 to 2005 showing the change in channel flow and active aggradation across the alluvial fan. After Davies et al. (2005).

values from Table 4, and for bedload yield show that this may vary from  $13 \text{ km}^2$  to  $670 \text{ km}^2$ . Evidently, it is prudent to anticipate widespread substantial aggradation of flood plains and alluvial fans following an Alpine Fault earthquake.

Korup et al. (2004) estimated that net sediment delivery rates from 3 large landslides within the Southern Alps ranged from  $10^{-3}\text{--}10^{-4} \text{ km}^3 \text{ a}^{-1}$ ; applying this rate to the aftermath of an Alpine Fault earthquake suggests that aggradation may continue for many hundreds of years. This time is longer than the average recurrence interval for the Alpine Fault, however, suggesting that the landscape is permanently aggrading. This cannot be correct as few large alluvial fans in the South Island are currently aggrading – most have incised fan heads indicating that past aggradation has ceased. One of the landslides studied by Korup et al. (2004) was generated by a  $M_w = 7.1$  earthquake. An Alpine Fault earthquake is expected to be an order of magnitude larger than this and will therefore generate a much larger amount of sediment ( $20\times$  more according to Eq. 9). This may result in the net

sediment delivery rates also being much higher and aggradation is therefore anticipated to last decades rather than centuries. A further explanation for faster delivery rates may be that much of the sediment available in small, steep catchments is (re)mobilised as debris flows, as we discuss next.

#### 4.7 Debris flows

The occurrence of debris flows in a given catchment requires a high Melton ratio (Jackson et al., 1987), sufficient available sediment, and large rainfall. The Melton ratio is an index of basin gradient and a high value requires a high relief combined with a small catchment area (Jackson et al., 1987). Previously unpublished data by O. Korup (University of Potsdam, personal communication, 2011) (Fig. 9) show that at least 77 catchments in the central Southern Alps have Melton ratios sufficient for the formation of debris flows.

The volume of debris flows is typically small compared to landslides (Table 5) with large flows having  $> 100\,000\text{ m}^3$  material (Pierson, 1980; McSaveney et al., 2005). From Eq. (8) we expect there to be  $0.4\text{--}4.2 \times 10^9\text{ m}^3$  (Table 4) of sediment available, which could translate to between 4000 and 42 000 debris flows of  $\sim 100\,000\text{ m}^3$ . This assumes that all of this sediment is (re)mobilised as debris flows, which is unlikely. Table 5 shows the percentage of landslide material involved in a set of debris flows after the 2008 Wenchuan earthquake. Taking the average of these (ignoring data from Zoumaling gully branches 2, 3, and 4 which appear to be anomalous) suggests that  $\sim 1/5$  of landslide deposits are involved in debris flows. If this were to be the case for New Zealand then the number of debris flows reduces to between  $\sim 1000$  and  $10\,000$  with volumes of  $\sim 100\,000\text{ m}^3$ .

The 2008  $M_w = 8.0$  Wenchuan earthquake generated  $> 56\,000$  landslides (Parker et al., 2011; Dai et al., 2011; Gorum et al., 2011) in the Longmen Shan mountains. Estimated volumes of debris range from  $0.1\text{--}2 \times 10^9$  (Dai et al., 2011) to  $5\text{--}15 \times 10^9\text{ m}^3$  (Parker et al., 2011). During the period 12–14 August 2010, long periods of rainfall resulted in a series of debris flows in the vicinity of Qingping town and Yingxiu City (Tang et al., 2011; Xu et al., 2012). In Qingping town 95 mm of rain fell in 12 h, and reports suggest this may have been higher in the mountains (Xu et al., 2012). This resulted in many debris flows forming simultaneously from the loose landslide material available (Table 5). As a result, the entire town of Qingping (an area of  $140 \times 10^4\text{ m}^2$ ) was buried, 14 people were killed, 33 injured, and  $> 370$  buildings destroyed. In Yingxiu City 162.1 mm of rain fell over 33 h (Xu et al., 2012). It resulted in  $\sim 21$  individual debris flows which combined and became hyperconcentrated flows, blocking the Minjiang River on the banks of which Yingxiu City stands (Tang et al., 2011). In both instances, the amount of rain that fell was not unusual for the region; however, the duration was considerably longer than is usual.

Heavy, long-duration rainstorms are frequent in the South Island, especially on the West Coast. It is therefore likely

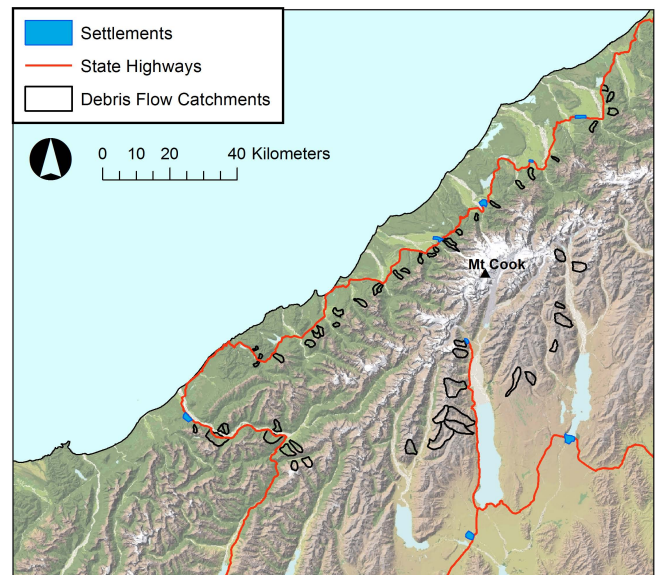


**Fig. 9.** River catchments in the central Southern Alps capable of generating debris flows.

**Table 5.** Volume comparison of landslide deposits generated by the 2008 Wenchuan earthquake and rainfall induced debris flows resulting from these deposits, during the 2010 rainstorm events from Qingping and Zoumaling catchments. Adapted from Xu et al. (2012).

Catchment/Gully	Landslide volume ( $10^4\text{ m}^3$ )	Debris flow volume ( $10^4\text{ m}^3$ )	Involved in debris flow (%)
Zoumaling*	432.7	82.0	19
Branch 1	7.0	2.0	29
Branch 2	1.8	1.5	83
Branch 3	1.1	3.0	272
Branch 4	3.8	2.0	53
Branch 5	73.2	20.0	27
Branch 6	46.6	13.0	28
Branch 7	26.2	7.0	27
Luojia	130.8	16.0	12
Dongzi	4.4	1.2	27
Wawa	40.2	9.8	24
Didong	3.2	0.7	22
Wenjia	5000.0	450.0	9
Linjia	7.8	1.5	19
Taiyang	8.6	2.0	23
Maliuwan	8.3	1.3	16
Pujia	10.0	0.8	8
Candum	10.3	2.4	23

\* Zoumaling catchment consisted of debris flows in 7 separate gullies with additional material being entrained in the main gully.

that the time between an Alpine Fault earthquake and the next rainstorm will be short, giving rivers very little time to redistribute the loose sediment. It is therefore conceivable

that most catchments in the Southern Alps with a sufficient Melton ratio, and in which landsliding occurred, could also generate debris flows in the first rainstorm after the event.

#### 4.8 Tsunami

As the 2004 Sumatra and 2011 Japan disasters showed, large tsunami can be catastrophic, resulting in tens-to-hundreds of thousands of deaths. Despite the Alpine Fault being neither a mega-thrust nor an offshore fault, instances of tsunami in the Tasman Sea perhaps related to Alpine Fault events may have been identified. Evidence from the Okarito lagoon in West Coast region suggests that this was once briefly flooded. Nichol et al. (2007) used trenching and coring techniques within the lagoon and identified features they described as typical of a tsunami event.  $C^{14}$  dating of an in situ buried bivalve dates this event to the mid-15th century, roughly when the ca. AD 1460 Alpine Fault event occurred (Nichol et al., 2007). Because the Alpine Fault is mainly onshore and dominantly strike slip in character, coastal tsunami are most likely to be generated by coseismic sediment slumps in offshore canyon heads. However, what Nichol et al. (2007) identified as a tsunami deposit may alternatively be a liquefaction deposit. Lagoons like Okarito are highly susceptible to liquefaction under intense shaking and it is almost certain the Okarito lagoon will have experienced high intensity shaking during all Alpine Fault events. Furthermore, no evidence of tsunami deposits from the same time have been found anywhere along the West Coast.

However, the South Island, and especially the Alpine region, have large lakes and fiords that are surrounded by steep rock slopes and are therefore susceptible to rockfall-initiated tsunamis. Thus while it appears unlikely that a catastrophic Tasman Sea tsunami will follow an Alpine Fault earthquake, the possibility of landslide-induced tsunami occurring in one or more of the South Island's lakes and fiords is of serious concern. Most of Fiordland's fiords are remote and unpopulated, however Milford Sound, which lies close to the Alpine Fault, is a popular tourist destination and averages > 1000 visitors a day. Analysis of swath bathymetry suggests as many as 20 large ( $\geq 10^7 \text{ m}^3$ ) rockfall deposits on the bed of Milford Sound which must post-date deglaciation of the fiord about 16 ka ago (Dykstra, 2012). Each of these is thought to have had the potential to cause a several-metre-scale tsunami. There are numerous other potential locations around the South Island including Lake Wakatipu by which the major tourist town of Queenstown is located.

One of the better known examples of rockfall-generated tsunami occurred at Lituya Bay, Alaska. A  $M_w = 8.3$  earthquake on the Fairweather Fault (Tocher, 1960; Fritz et al., 2009) generated a landslide with a volume of  $\sim 30.6 \times 10^6 \text{ m}^3$  and total fall height of  $\sim 915 \text{ m}$  into Lituya Bay (Miller, 1960; Fritz et al., 2009). This caused a mega-tsunami, which travelled at speeds of  $150\text{--}200 \text{ km h}^{-1}$  and swept 11 km to the mouth of the bay (Miller, 1960). On a spur

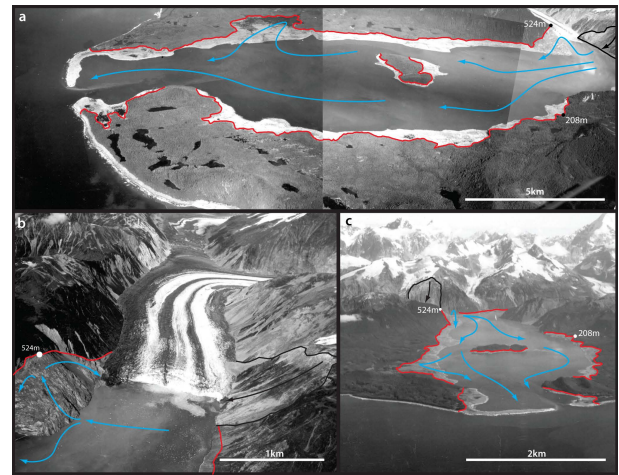


**Fig. 10.** Lituya Bay following the 1958 tsunami. (a) NW panoramic view of Lituya Bay and Centoaph Island; (b) NW view of Gilbert Inlet and Lituya Glacier showing landslide scar and wave run-up on spur opposite landslide; (c) NE view of Lituya Bay. Photos from USGS.

immediately opposite the landslide source, at a distance of  $\sim 1.3 \text{ km}$ , the wave ripped trees from the ground and eroded soil down to bedrock up to a height of 524 m above water level (Fig. 10) (Miller, 1960; Fritz et al., 2009): this is to date the highest known tsunami run-up ever generated. In total, over  $10 \text{ km}^2$  of forest was destroyed along the bay shoreline (Fig. 10), 2 boats were sunk and 2 people were killed (Miller, 1960).

At its closest point, Lituya Bay lies  $< 1 \text{ km}$  from the trace of the Fairweather Fault rupture (Stauder, 1960). Similarly, the Alpine Fault runs in close proximity to Milford Sound, running offshore  $< 5 \text{ km}$  north of the fiord. We have suggested that rupture of the Alpine Fault may occur on the full length of the fault and will therefore be  $< 5 \text{ km}$  from Milford Sound. Milford Sound has already been shown to have sustained large rockfalls and possibly tsunamis. Given the similarities, a Lituya Bay-type tsunami in Milford Sound cannot be considered improbable.

#### 4.9 Liquefaction

Liquefaction typically affects saturated, loose, sandy/silty soils which settle and compress under intense shaking causing fluids and silts within the soils to rise towards the surface. Hancox et al. (1997) found that throughout New Zealand the intensity threshold for liquefaction was MM VII for sand boils, and MM VIII for lateral spreading; however, it is possible for both to occur one level lower in particularly susceptible materials. Following the 2011  $M = 9.0$  Tohoku earthquake, significant liquefaction occurred in the Kanto area of Tokyo, 400 km from the epicentre (Bhattacharya et al., 2011). This is believed to have been caused by long-duration MM VI or lower shaking (Bhattacharya et al., 2011).

Christchurch experienced multiple liquefaction events following a series of  $M > 6$  earthquakes in 2010 and 2011 (Cubrinovski et al., 2011). Similarly, historic liquefaction has been recorded in numerous susceptible locations in Canterbury following significant earthquakes (Table 1). These locations are  $< 150$  km from the Alpine Fault, and are anticipated to receive MM VI+ shaking (Fig. 5).

Analyses of the West Coast region by McCahon et al. (2005, 2006a, b) have determined a number of locations that could potentially liquefy following an Alpine Fault earthquake. McCahon et al. (2005) analysed the likely hazards associated with an Alpine Fault earthquake for Grey District and determined from geological and historical evidence that liquefaction was likely to occur in a number of places. These included the swampy areas of large lakes, around the river estuary in Greymouth, and at a number of small coastal settlements. Applying the same analysis to Buller District, McCahon et al. (2006b) found that significant liquefaction was likely to occur in the major coastal town of Westport as well as much smaller inland settlements located on river flood plains. McCahon et al. (2006a) further identified the large coastal town of Hokitika as a likely location for liquefaction. Significant settlements that have a similar geology and/or previous evidence of liquefaction, and are therefore considered potential liquefaction sites include Invercargill, Gore, and Christchurch.

#### 4.10 Glacial advance

The supraglacial deposits of large landslides falling onto glaciers can significantly alter glacier behaviour by adding extra mass to the glacier and by reducing ice-surface ablation (Tarr and Martin, 1912; Schulmeister et al., 2009; Reznichenko et al., 2011). Debris depths of  $\sim 1$  m appear to be sufficient to significantly suppress surface ablation to cause glacial advance if rock-avalanche debris covers more than about 10 % of the glacier ablation zone area (Schulmeister et al., 2009; Reznichenko et al., 2011). This effect was first described by Tarr and Martin (1912) when they noted that several glaciers in Yakutat Bay, Alaska, had advanced following a series of large earthquakes in the region in 1899. Following the 1964 great Alaskan earthquake, a substantial landslide covered  $\sim 50$  % of the ablation zone of the Sherman Glacier leading to an 80 % reduction in surface ablation (McSaveney, 1975). This resulted in the glacier changing from a retreat phase to a slow advance phase, which was continuing  $\sim 40$  yr later (Reznichenko et al., 2011). In 1986, a landslide in the Karakoram region of the Himalayas covered 15–20 % of the Baultar Glacier ablation zone which resulted in the glacier surging for the first 2 yr and then continuing to advance  $\sim 2$  km for a further 12 yr (Hewitt, 2009).

Despite the Southern Alps hosting  $> 3000$  glaciers (Chinn, 2001), most of these are smaller than the anticipated average earthquake-generated landslide size ( $\sim 25\,000$  m<sup>3</sup>). Landslides falling onto such small glaciers are unlikely to

have a significant effect. Of more concern are landslides falling onto the major glaciers of the South Island. These cover a total area of 245 km<sup>2</sup> (Chinn, 2001), which is about 1 % of the area likely to be affected by landsliding (Table 4). However, the risk of landsliding onto one of these glaciers is likely higher than this suggests as each glacier is situated in a steep sided valley  $< 20$  km from the Alpine Fault.

Reznichenko et al. (2011) estimated that an 80 % reduction in ablation would be sufficient to cause the Franz Josef Glacier to advance  $\sim 6$  km. Schulmeister et al. (2009) estimated that given such a scenario, the glacier could reach the township within 3–6 yr. Similar effects are anticipated for each of the major glaciers should a large landslide impact them. Each of these glaciers is a popular tourist destination and as a result have townships and highways down valley. Additionally, previous advances have caused severe aggradation in proglacial rivers and it is currently not known how much aggradation a large-scale advance might cause – but it would certainly be sufficient to significantly alter river behaviour.

#### 4.11 Catastrophic glacier multi-phase mass movement

Catastrophic glacier multi-phase mass movements are rare events that have been recorded infrequently. They involve collapse of all or part of a glacier due to significant rock avalanching and involve extraordinary velocities, long-distance run-outs, and superelevations (Petraikov et al., 2008). From the few examples studied, they begin as rock and/or ice avalanches/slides before gradually transforming into ultra-high speed flows ( $> 30$  ms<sup>-1</sup>) and often finish as debris flows (Huggel et al., 2005; Petraikov et al., 2008). They can travel for distances of tens of kilometres (Huggel et al., 2005; Petraikov et al., 2008).

The most catastrophic glacier multi-phase mass movement on record is the 2002 Kolka-Karmadon event which occurred in North Ossetia, Russia and killed  $\sim 140$  people. The main part of the glacier detached during a major rock avalanche and cascaded down the valley for a total distance of  $\sim 20$  km, at which point a mudflow was generated flowing a further 15–17 km downstream. The average velocity of the main flow is thought to have been close to 50 ms<sup>-1</sup> (180 km h<sup>-1</sup>) (Petraikov et al., 2008) with maximum velocity estimates ranging from 70 ms<sup>-1</sup> (250 km h<sup>-1</sup>) (Drobyshev, 2006) to 90 ms<sup>-1</sup> (325 km h<sup>-1</sup>) (Huggel et al., 2005). Until this event collapse of an entire valley-type glacier had not been considered possible.

No evidence for a similar event has yet been identified anywhere in New Zealand. This may be because such an event has never occurred in New Zealand or because evidence has yet to be identified. Nevertheless, given that these events are so rare, and the lack of historical evidence, it seems unlikely, but possible, that such an event would occur following a great Alpine Fault earthquake.

## 5 Discussion

### 5.1 Importance of landsliding

Many of the estimates presented above are dependent on the size and distribution of landsliding. In order for each of the other geomorphic consequences (excluding liquefaction) to take place a landslide must first occur. However, accurately predicting the locations of landsliding resulting from an earthquake is fraught with difficulties. In order to assess where such landsliding might occur one would need to know (or accurately predict) the epicentral location, peak ground acceleration, topographic amplification of each mountain, slope angle, rock type, rock strength etc. This still would only provide a susceptibility map, which would not necessarily identify where landslides will occur, only where they are most likely. While producing such a map is possible in principle, it is presently impracticable. We have therefore attempted to demonstrate the likely order of magnitude of landsliding and use these results to determine the orders of magnitude of the consequential geomorphic effects.

Our estimates for landsliding are calculated from statistical relationships of Malamud et al. (2004) and Keefer and Wilson (1989). They present estimated average values for a  $M_w = 8.0$  earthquake based on well studied historical earthquakes throughout the world. Since an Alpine Fault earthquake is not included in the data used to determine these estimates, there is the potential that Alpine Fault events behave very differently, resulting in larger or smaller values. Nonetheless, there is no direct evidence to suggest that an Alpine Fault earthquake would be such an outlier, therefore the results of Malamud et al. (2004) and Keefer and Wilson (1989) provide useful, order-of-magnitude estimates of the likely scale of events that may result from an Alpine Fault earthquake.

### 5.2 Wenchuan earthquake

In this review we have referred to various examples of geomorphic consequences resulting from the 2008 Wenchuan earthquake. That earthquake occurred on a major fault system, was  $M_w = 8.0$ , involved oblique-right-lateral motion with  $\sim 6$  m lateral and  $\sim 1$  m vertical slip, and had a surface rupture  $> 200$  km long. Furthermore, the environment that this earthquake occurred in is mountainous, and heavily vegetated. In all these respects, it is similar to the Southern Alps and to the anticipated Alpine Fault earthquake. We therefore suggest the 2008 Wenchuan event to be a plausible generic analogue for a future Alpine Fault earthquake. Comparisons made between the two events herein are highlighted to demonstrate the likely scale of consequential geomorphic events. There will of course be specific differences due to lithology. The Longmenshan Mountains where the Wenchuan earthquake occurred are composed primarily of Devonian to Triassic carbonates with granitic basement

rock. The Southern Alps in comparison, consist of schists and greywacke and this may have an influence on the degree of landsliding.

One key difference that should be noted is the seasonality of rainfall in the Wenchuan area. The majority of annual rainfall in Wenchuan falls between May and September and this is likely to have affected the time delay in debris flow formation. The earthquake occurred in May and heavy rainstorms during the wet season did cause several debris flows however, the most significant flows did not occur until 2 yr after the event, when the first unusually long-duration post-earthquake rainfall occurred. This may explain why only 21 % of landslide material (Table 5) generated debris flows. River systems had reworked and redistributed sediment over 2 yr, reducing the amount available for debris flows. However, there is no wet season in New Zealand, and the first long-duration rainstorm is likely to occur soon after an Alpine Fault earthquake. Rivers may not, in that case, have had enough time to redistribute landslide deposits significantly and a larger percentage of material may be available to form debris flows. This may present itself as larger numbers of debris flows than anticipated, or by debris flows containing larger volumes of sediment. Debris flows may also have a significant impact on aggradation. Debris flows will transport large volumes of loose landslide sediment from small river catchments and deposit them further down valley, closer to, or possibly on, larger alluvial fans and floodplains. This could accelerate aggradation, as sediment will be easier to rework and redistribute by rivers and will have a much shorter distance to travel to the alluvial fan. In this case, areas experiencing large debris flows will likely have aggradation lasting less than the anticipated several decades, or will experience a larger amount of aggradation in the short-term than areas not sustaining debris flows.

### 5.3 The 1855 Wairarapa earthquake: a New Zealand analogue

Despite the high seismicity throughout New Zealand, only one great ( $M > 8$ ) earthquake has occurred in the region since European settlement (Table 1). This is the 1855 Wairarapa earthquake which occurred in the lower North Island on the Wairarapa Fault and is thought to have been  $M_w = 8.1$ – $8.4$  (Grapes and Downes, 1997; Little and Rodgers, 2004). The epicentre of this earthquake is thought to have been near to Wellington (Grapes and Downes, 1997) and rupture most likely propagated in both directions totalling  $> 140$  km (Ongley, 1943). Measured lateral displacement along the fault rupture has been shown to be the largest known for historic earthquakes globally, reaching 18.7 m (Little and Rodgers, 2004). Shaking intensity is inferred to have reached MM X in the epicentral region, similar to the 1929 Buller, and 1968 Inangahua earthquakes (Dowrick, 2005).

Hancox (2005) reported that significant landsliding occurred as a result of this earthquake in the Rimutaka ranges due to the presence of sheared greywacke rocks, steep slopes, and the location close to, and on the upthrown side of the Wairarapa Fault (Hancox, 2005). In all these respects the Rimutaka Ranges are similar to the Southern Alps. Grapes and Downes (1997) suggest that landsliding affected an area of 52 000 km<sup>2</sup> possibly extending out to 135 000 km<sup>2</sup>. We note that this corresponds well to Eq. (7) which for a  $M = 8.2$  earthquake suggests a mean landslide affected area of  $\sim 54\,000$  km<sup>2</sup> and a maximum of  $\sim 164\,000$  km<sup>2</sup>. Hancox (2005) reported that some of the largest landslides in the Rimutaka ranges were reactivated by a rainstorm in 2005, 150 yr after the earthquake.

The largest landslide reported from this earthquake, the Hidden Lakes landslide, was  $\sim 11 \times 10^6$  m<sup>3</sup> (Hancox, 2005), much smaller than that suggested by Eq. (11). This may suggest that the Wairarapa earthquake was an extreme event, generating landslides much smaller than anticipated despite affecting an area consistent with empirical formulae. The Hidden Lakes landslide blocked the Ruamahanga River and several lakes formed behind the dam (Hancox, 2005). This dam partially failed sometime after the earthquake, and the resulting dam-break flood destroyed a downstream Māori Pā (village) (Grapes, 1988). Some of the lakes that had formed behind however, remained intact and as of 2013 still exist, resulting in long-term downstream hazard like that caused by the Young River landslide dam in the South Island.

As well as landsliding this event is known to have caused substantial liquefaction, seiches, and tsunamis. Liquefaction is reported to have occurred in numerous susceptible locations in the lower North Island and upper South Island (Grapes and Downes, 1997; Hancox, 2005). Seiches, the oscillation of confined or semi-confined water bodies, are reported to have occurred at many locations across the entire country including several lakes and rivers in the North Island as well as some bays and rivers in the South Island (Grapes and Downes, 1997; Downes, 2005). Tsunami's were recorded at several locations around the country with the largest recorded run-up (10 m) occurring where the Wairarapa Fault runs offshore (Downes, 2005). High intensity shaking is known to have caused submarine landsliding in the Cook Strait which separates the North and South Islands (Grapes and Downes, 1997) and may have been sufficient to cause tsunami. However, the Wairarapa Fault rupture is known to have occurred partly offshore in the Strait, and uplift on the fault is sufficient to have generated the tsunami. Grapes and Downes (1997) and Downes (2005) therefore attribute this tsunami to uplift along the fault rather than submarine landsliding.

Given that such numerous and widespread geomorphic effects are known to have occurred as the result of a great earthquake in New Zealand previously, it seems likely that a great earthquake on the Alpine Fault will generate similarly numerous and widespread effects. Nevertheless, many of the

effects detailed throughout this review represent a worst-case scenario and it is unlikely, but not impossible, that all effects will reach such magnitudes. We suggest it is most likely that some of these effects will reach their worst-case potential, while others will occur at some magnitude below this. It is not, however, possible to say which effects will reach this potential and it is because of this that we demonstrate such scenarios for each effect. Despite this we also acknowledge the fact that these worst-case scenarios are determined from historic examples, for which often the geologic record is incomplete. This may result in what is currently deemed worst-case being exceeded as was witnessed in the 2011 Japan tsunami and other events. Nevertheless, lack of geologic evidence for the occurrence of larger events precludes us from suggesting events larger than those previously witnessed.

## 6 Summary

There is 85 % probability in the next century that the Alpine Fault will rupture causing a  $M_w = 8.0+$  earthquake. We suggest that a most likely location for epicentre is on the central segment of the fault, possibly in the Mt Cook region. Rupture is then likely to involve the entire 480 km length of the fault. Maximum Mercalli shaking intensity will reach at least MM X close to the fault with local conditions along the fault trace possibly producing MM XI or XII. The entire South Island will experience MM V or greater shaking. The largest-magnitude aftershock is anticipated to occur within one year of the main shock and is likely to be  $M_w \sim 7.0$  but could range from  $M_w = 5.0-8.0$ . More than ten  $M_w = 6.0+$  earthquakes are expected in the total aftershock sequence. Total landslide volume is likely to exceed 1 billion m<sup>3</sup> and affect an area of more than 30 000 km<sup>2</sup>. Landslide dams, dam-break floods and associated river response are expected to occur throughout this region. Figure 7 shows a number of most likely river catchments to be affected. The Young river landslide dam could fail, resulting in a dam-break flood. Landslide-generated tsunami pose hazards in alpine lakes and fiords especially Milford Sound. Long duration rainfall events following the earthquake will mobilise landslide debris in the form of debris flows which may number  $> 1000$  individual flows. These are likely to occur over several years as continuing landsliding and aftershock processes add to the available sediment. River aggradation of some metres depth is likely to cover an area of tens to hundreds of square kilometres and to continue for several decades. Long-duration low-frequency shaking may induce liquefaction in many locations including Christchurch, Greymouth, Hokitika and Invercargill. Landsliding onto any of the large glaciers of the Southern Alps may induce glacial advance of several kilometres. The effect this will have on proglacial river aggradation is currently unknown, but is likely to be significant. Nevertheless, the environment will recover and return to its current condition in relatively short time. Evidence of previous Alpine Fault earthquakes is not immediately obvious in the

landscape and often difficult to identify due to such recovery. Within 50 yr, evidence of the event within the environment will be greatly reduced and within 100 yr evidence will be limited to just a few, small, exceptional locations.

*Acknowledgements.* We would like to thank Theodosios Kritikos for his helpful comments and discussions throughout the compilation of this review as well as his in-depth knowledge on the available literature. We also thank Oliver Korup for allowing us to use his data on debris flows. Finally we thank Riccardo Caputo and the two anonymous reviewers whose helpful criticisms helped focus and improve this review.

Edited by: F. Guzzetti

Reviewed by: R. Caputo and two anonymous referees

## References

- Adams, J.: Contemporary uplift and erosion of the Southern Alps, New Zealand: Summary, *Geol. Soc. Am. Bull.*, 91, 2–4, 1980a.
- Adams, J.: Paleoseismicity of the Alpine fault seismic gap, New Zealand, *Geology*, 8, 72–76, 1980b.
- Adams, J.: Earthquake-dammed lakes in New Zealand, *Geology*, 9, 215–219, 1981.
- Anderson, H., Beanland, S., Blick, G., Darby, D., Downes, G., Haines, J., Jackson, J., Robinson, R., and Webb, T.: The 1968 May 23 Inangahua, New Zealand, earthquake: an integrated geological, geodetic, and seismological source model, *New Zeal. J. Geol. Geop.*, 37, 59–86, 1994.
- Beavan, J., Moore, M., and Pearson, C.: Crustal deformation during 1994–1998 due to oblique continental collision in the central Southern Alps, New Zealand, and implications for seismic potential of the Alpine fault, *J. Geophys. Res.*, 104, 233–255, 1999.
- Beavan, J., Samsonov, S., Denys, P., Sutherland, R., Palmer, N., and Denham, M.: Oblique slip on the Puysegur subduction interface in the 2009 July  $M_W$  7.8 Dusky Sound earthquake from GPS and InSAR observations: implications for the tectonics of southwestern New Zealand, *Geophys. J. Int.*, 183, 1265–1286, 2010a.
- Beavan, J., Denys, P., Denham, M., Hager, B., Herring, T., and Molnar, P.: Distribution of present-day vertical deformation across the Southern Alps, New Zealand, from 10 years of GPS data, *Geophys. Res. Lett.* 37, 7–11, 2010b.
- Beavan, J., Fielding, E., Motagh, M., Samsonov, S., and Donnelly, N.: Fault Location and Slip Distribution of the 22 February 2011  $M_w$  6.2 Christchurch, New Zealand, Earthquake from Geodetic Data, *Seismol. Res. Lett.*, 82, 789–799, doi:10.1785/gssrl.82.6.789, 2011.
- Becker, J. S., Johnston, D. M., Paton, D., Hancox, G. T., Davies, T. R. H., McSaveney, M. J., and Manville, V. R.: Response to Landslide Dam Failure Emergencies: Issues Resulting from the October 1999 Mount Adams Landslide and Dam-Break Flood in the Poerua River, Westland, New Zealand, *Nat. Hazards*, 8, 35–42, doi:10.1061/(ASCE)1527-6988(2007)8:2(35), 2007.
- Berril, J. B., Mulqueen, P. C., and Ooi, E. T. C.: Liquefaction of Kaiapoi in the 1901 Cheviot, New Zealand, earthquake, *Bulletin of the New Zealand National Society of Earthquake Engineering*, 27, 178–189, 1994.
- Berryman, K. and Villamor, P.: Surface rupture of the Poulter Fault in the 1929 March 9 Arthur's Pass earthquake, and redefinition of the Kakapo Fault, New Zealand, *New Zeal. J. Geol. Geop.*, 47, 341–351, 2004.
- Berryman, K., Beanland, S., Cooper, A. F., Cutten, H. N., Norris, R. J., and Wood, P. R.: The Alpine Fault, New Zealand: variation in Quaternary tectonic style and geomorphic expression, *Annales Tectonicae*, VI, 126–163, 1992.
- Berryman, K., Alloway, B. S., Almond, P., Barrell, D., Duncan, R. P., McSaveney, M. J., Read, S., and Tonkin, P.: Alpine fault rupture and landscape evolution in Westland, New Zealand, in: *Proceedings 5th International Conference of Geomorphology*, Tokyo, 2001.
- Berryman, K., Cooper, A. F., Norris, R. J., Villamor, P., Sutherland, R., Wright, T., Schermer, E., Langridge, R., and Biasi, G.: Late Holocene Rupture History of the Alpine Fault in South Westland, New Zealand, *B. Seismol. Soc. Am.*, 102, 620–638, 2012.
- Bhattacharya, S., Hyodo, M., Goda, K., Tazoh, T., and Taylor, C. A.: Liquefaction of soil in the Tokyo Bay area from the 2011 Tohoku (Japan) earthquake, *Soil Dyn. Earthq. Eng.*, 31, 1618–1628, 2011.
- Bouchon, M. and Vallée, M.: Observation of Long Supershear Rupture During the Magnitude 8.1 Kunlunshan Earthquake, *Science*, 301, 824–826, 2003.
- Bourne, S. J., Arnadottir, T., and Beavan, J.: Crustal deformation of the Marlborough fault zone in the South Island of New Zealand: Geodetic constraints over the interval 1982–1994, *J. Geophys. Res.*, 103, 30147–30165, doi:10.1029/98JB02228, 1998.
- Bull, W. B.: Prehistorical earthquakes on the Alpine fault, New Zealand, *J. Geophys. Res.*, 101, 6037–6050, doi:10.1016/0148-9062(94)92684-0, 1996.
- Bull, W. B.: Lichenometry dating of coseismic changes to a New Zealand landslide complex, *Ann. Geophys.-Italy*, 46, 1155–1167, 2003.
- Chinn, T. J.: Distribution of the glacial water resources of New Zealand, *J. Hydrol. (New Zealand)*, 40, 139–187, 2001.
- Cooper, A. F.: Retrograde Alteration of Chromian Kyanite in Metachert and Amphibolite Whiteschist from the Southern Alps, New Zealand, with Implications for Uplift on the Alpine Fault, *Miner. Petrol.*, 75, 153–164, doi:10.1007/BF00389775, 1980.
- Cooper, A. F. and Norris, R. J.: Estimates for the timing of the last coseismic displacement on the Alpine fault, northern Fiordland, New Zealand, *New Zeal. J. Geol. Geop.*, 40, 303–307, 1990.
- Costa, J. E. and Schuster, R. L.: The formation and failure of natural dams, *Geol. Soc. Am. Bull.*, 100, 1054–1068, 1988.
- Costa, J. E. and Schuster, R. L.: Documented Historical Landslide Dams from Around the World: U.S. Geological Survey Open-File Report 91-239, 490 pp., 1991.
- Coulter, R. F.: Tectonic Geomorphology and Seismic Hazard of the Mt Fyffe section of the Hope fault, MSc. Thesis, University of Canterbury, 2007.
- Cowan, H. A.: Late Quaternary displacements on the Hope Fault at Glynn Wye, North Canterbury, New Zeal. *J. Geol. Geop.*, 33, 285–293, 1990.
- Cowan, H. A.: The North Canterbury earthquake of September 1, 1888, *J. Roy. Soc. New Zeal.*, 21, 1–12, 1991.
- Cowan, H. A.: Structure, seismicity and tectonics of the Porter's Pass-Amberley fault zone, North Canterbury, New Zealand, Ph.D. thesis, University of Canterbury, 247 pp., 1992.

- Cowan, H. A. and McGlone, M. S.: Late Holocene displacements and characteristic earthquakes on the Hope River segment of the Hope fault, New Zealand, *J. Roy. Soc. New Zeal.*, 21, 373–384, 1991.
- Cubrinovski, M., Bray, J. B., Taylor, M., Giorgini, S., Bradley, B., Wotherspoon, L., and Zupan, J.: Soil Liquefaction Effects in the Central Business District during the February 2011 Christchurch Earthquake, *Seismol. Res. Lett.*, 82, 893–904, 2011.
- Dai, F. C., Xu, C., Yao, X., Xu, L., Tu, X. B., and Gong, Q. M.: Spatial distribution of landslides triggered by the 2008 Ms 8.0 Wenchuan earthquake, China, *J. Asian Earth Sci.*, 40, 883–895, doi:10.1016/j.jseas.2010.04.010, 2011.
- Davey, F. J., Henyey, T., Kleffmann, S., and Melhuish, A.: Crustal reflections from the Alpine Fault Zone, South Island, New Zealand, *New Zeal. J. Geol. Geop.*, 38, 37–41, 1995.
- Davies, T. R. H.: Landslide-dambreak floods at Franz Josef Glacier township, Westland, New Zealand: a risk assessment, *J. Hydrol (New Zealand)*, 41, 1–17, 2002.
- Davies, T. R. H. and Korup, O.: Persistent alluvial fanhead trenching resulting from large, infrequent sediment inputs, *Earth Surf. Proc. Land.*, 32, 725–742, doi:10.1002/esp, 2007.
- Davies, T. R. H. and McSaveney, M. J.: Runout of rock avalanches and volcanic debris avalanches (Invited Keynote Lecture), in: Proceedings of the international conference on fast slope movements: prediction and prevention for risk mitigation, edited by: Piceralli, L., Pàtron, Naples, 2006.
- Davies, T. R. H. and Scott, B. K.: Dambreak flood hazard from the Callery River, Westland, New Zealand, *J. Hydrol (New Zealand)*, 36, 1–13, 1997.
- Davies, T. R. H., McSaveney, M. J., and Doscher, C.: Monitoring and effects of landslide-induced aggradation in the Poerua Valley, Westland, EQC Report, Project No. 03/499, 2005.
- Davies, T. R. H., Manville, V., Kunz, M., and Donadini, L.: Modelling landslide dambreak flood magnitudes: a case study, *J. Hydrol. Eng.*, 133, 713–720, 2007.
- DeMets, C., Gordon, R. G., Argus, D. F., and Stein, S.: Effect of recent revisions to the geomagnetic reversal timescale on estimates of current plate motions (Paper 94GL02118), *Geophys. Res. Lett.*, 21, 2191–2194, doi:10.1029/94GL02118, 1994.
- De Pascale, G. P. and Langridge, R. M.: First direct geological evidence of a great earthquake in 1717, central Alpine Fault, New Zealand, *Geology*, 2012.
- Downes, G. L.: The 1855 January 23 M8+ Wairarapa earthquake – what contemporary accounts tell us about it, in: The 1855 Wairarapa Earthquake Symposium, Wellington, New Zealand, 8–10 September 2005, 1–11, 2005.
- Dowrick, D. J.: Damage and intensities in the M7.8 1929 Murchison, New Zealand, earthquake, *Bulletin of the New Zealand National Society for Earthquake Engineering*, 27, 190–204, 1994.
- Dowrick, D. J.: Strong ground shaking in the 1855 Wairarapa earthquake, in: The 1855 Wairarapa Earthquake Symposium, Wellington, New Zealand, 8–10 September 2005, 79–83, 2005.
- Drobyshev, V. N.: Glacial catastrophe of 20 September 2002 in North Osetia, *Russian Journal of Earth Sciences*, 8, 1–25, doi:10.2205/2006ES000207, 2006.
- Dykstra, J.: The role of mass wasting and ice retreat in the post-LGM evolution of Milford Sound, Fiordland, New Zealand, Ph.D. thesis, University of Canterbury, New Zealand, 2012.
- Fritz, H. M., Mohammed, F., and Yoo, J.: Lituya Bay Landslide Impact Generated Mega-Tsunami 50th Anniversary, *Pure Appl. Geophys.*, 166, 153–175, doi:10.1007/s00024-008-0435-4, 2009.
- Gage, M.: Rocks and Landscape, in: *The Natural History of Canterbury*, edited by: Knox, G. A., Reed, A. H., and Reed, A. W., Canterbury University Press, 25–43, 1969.
- GNS Science: available at: <http://info.geonet.org.nz/display/slide/Young+River+Landslide>, last access: 27 November 2012.
- Gledhill, K., Ristau, J., Reyners, M., Fry, B., and Holden, C.: The Darfield (Canterbury, New Zealand) Mw 7.1 Earthquake of September 2010: A Preliminary Seismological Report, *Seismol. Res. Lett.*, 82, 378–386, doi:10.1785/gssrl.82.3.378, 2011.
- Gorum, T., Fan, X., van Westen, C. J., Huang, R. Q., Xu, Q., Tang, C., and Wang, G.: Distribution pattern of earthquake-induced landslides triggered by the 12 May 2008 Wenchuan earthquake, *Geomorphology*, 133, 152–167, 2011.
- Grapes, R.: Geology and revegetation of an 1855 landslide, Ruamahanga River, Kopuaranga, Wairarapa, Tuatara, Wellington, 30, 77–83, 1988.
- Grapes, R. and Downes, G.: The 1855 Wairarapa, New Zealand, earthquake: analysis of historical data, *Bulletin of the New Zealand National Society for Earthquake Engineering* 30, 271–368, 1997.
- Grapes, R., Little, T., and Downes, G.: Rupturing of the Awatere fault during the 1848 October 16 Marlborough earthquake, New Zealand: historical and present day evidence, *New Zeal. J. Geol. Geop.*, 41, 387–399, 1998.
- Griffiths, G. A.: High sediment yields from major rivers of the Western Southern Alps, New Zealand, *Nature*, 282, 61–63, 1979.
- Hainzl, S., Zöller, G., and Kurths, J.: Self-organization of spatio-temporal earthquake clusters, *Nonlin. Processes Geophys.*, 7, 21–29, doi:10.5194/npg-7-21-2000, 2000.
- Hancox, G. T.: Landslides and liquefaction effects caused by the 1855 Wairarapa earthquake: then and now, in: The 1855 Wairarapa Earthquake Symposium, Wellington, New Zealand, 8–10 September 2005, 84–95, 2005.
- Hancox, G. T., Perrin, N. D., and Dellow, G. D.: Earthquake-induced landsliding in New Zealand and implications for MM intensity and seismic hazard assessment, *GNS Client Report*, 43601B, 1997.
- Hancox, G. T., McSaveney, M. J., Manville, V. R., and Davies, T. R. H.: The October 1999 Mt Adams rock avalanche and subsequent landslide dam-break flood and effects in Poerua River, Westland, New Zealand, *New Zeal. J. Geol. Geop.*, 48, 683–705, 2005.
- Hewitt, K.: Rock avalanches that travel onto glaciers and related developments, Karakoram Himalaya, Inner Asia, *Geomorphology*, 103, 66–79, doi:10.1016/j.geomorph.2007.10.017, 2009.
- Hewitt, K., Clague, J. J., and Orwin, J. F.: Legacies of catastrophic rock slope failures in mountain landscapes, *Earth-Sci. Rev.*, 87, 1–38, doi:10.1016/j.earscirev.2007.10.002, 2008.
- Hicks, D. M., Hill, J., and Shankar, U.: Variation of suspended sediment yields around New Zealand: the relative importance of rainfall and geology, *IAHS publication*, 236, 149–156, 1996.
- Holden, C.: Kinematic Source Model of the 22 February 2011 Mw 6.2 Christchurch Earthquake Using Strong Motion Data, *Seismol. Res. Lett.*, 82, 783–788, doi:10.1785/gssrl.82.6.783, 2011.

- Hovius, N., Stark, C., and Allen, P. A.: Sediment flux from a mountain belt derived by landslide mapping, *Geology*, 25, 231–234, doi:10.1130/0091-7613(1997), 1997.
- Howard, M., Nicol, A., Campbell, J., and Pettinga, J.: Recent Paleoearthquakes of the Porters Pass Fault and Hazard Posed to Christchurch, New Zealand, *Proceedings of the Pacific Conference on Earthquake Engineering*, 69, 1–8, 2003.
- Hsü, K. J.: Catastrophic debris streams (sturzstrom) generated by rockfalls, *Geol. Soc. Am. Bull.*, 86, 129–140, 1975.
- Huang, R., Pei, X., Fan, X., Zhang, W., Li, S., and Li, B.: The characteristics and failure mechanism of the largest landslide triggered by the Wenchuan earthquake, May 12, 2008, China, *Landslides*, 9, 131–142, 2011.
- Huggel, C., Zraggen-Oswald, S., Haerberli, W., Kääh, A., Polkvoj, A., Galushkin, I., and Evans, S. G.: The 2002 rock/ice avalanche at Kolka/Karmadon, Russian Caucasus: assessment of extraordinary avalanche formation and mobility, and application of Quick-Bird satellite imagery, *Nat. Hazards Earth Syst. Sci.*, 5, 173–187, doi:10.5194/nhess-5-173-2005, 2005.
- Hull, A. G. and Berryman, K.: Holocene tectonism in the region of the Alpine fault at Lake McKerrow, Fiordland, New Zealand, *Royal Society of New Zealand Bulletin*, 24, 317–331, 1986.
- Kamp, P. J. J. and Tippett, J. M.: Dynamics of Pacific Plate Crust in the South Island (New Zealand) Zone of Oblique Continent-Continent Convergence, *J. Geophys. Res.*, 98, 16105–16118, doi:10.1029/93JB01091, 1993.
- Kamp, P. J. J., Green, P. F., and White, S. H.: Fission track analysis reveals character of collisional tectonics in New Zealand, *Tectonics*, 8, 169–195, 1989.
- Keefer, D. K.: Landslides caused by earthquakes, *Geol. Soc. Am. Bull.*, 95, 406–421, 1984.
- Keefer, D. K. and Wilson, R. C.: Predicting earthquake-induced landslides with emphasis on arid and semi-arid environments, in: *Landslides in a Semi-Arid Environment with emphasis on the inland valleys of Southern California*, Volume No. 2, edited by: Sadler, P. M. and Morton, D. M., Inland Geological Society of Southern California Publications, Riverside, CA, 118–149, 1989.
- Korup, O.: Geomorphometric characteristics of New Zealand landslide dams, *Eng. Geol.*, 73, 13–35, doi:10.1016/j.enggeo.2003.11.003, 2004.
- Korup, O.: Geomorphic hazard assessment of landslide dams in South Westland, New Zealand: fundamental problems and approaches, *Geomorphology*, 66, 167–188, doi:10.1016/j.geomorph.2004.09.013, 2005.
- Korup, O. and Tweed, F.: Ice, moraine, and landslide dams in mountainous terrain, *Quaternary Sci. Rev.*, 26, 3406–3422, doi:10.1016/j.quascirev.2007.10.012, 2007.
- Korup, O., McSaveney, M. J., and Davies, T. R. H.: Sediment generation and delivery from large historic landslides in the Southern Alps, New Zealand, *Geomorphology*, 61, 189–207, doi:10.1016/j.geomorph.2004.01.001, 2004.
- Langridge, R., Campbell, J., Hill, N., Pere, V., Pope, J., Pettinga, J., Estrada, B., and Berryman, K.: Paleoseismology and slip rate of the Conway Segment of the Hope Fault at Greenburn Stream, South Island, New Zealand, *Ann. Geophys-Italy*, 46, 1119–1139, doi:10.4401/ag-3449, 2003.
- Leitner, B., Eberhart-Phillips, D., Anderson, H., and Nabelek, J. L.: A focused look at the Alpine fault, New Zealand: Seismicity, focal mechanisms, and stress observations, *J. Geophys. Res.*, 106, 2193–2220, doi:10.1029/2000JB900303, 2001.
- Li, Y., Gong, J. H., Zhu, J., Ye, L., Song, Y. Q., and Yue, Y. J.: Efficient dam break flood simulation methods for developing a preliminary evacuation plan after the Wenchuan Earthquake, *Nat. Hazards Earth Syst. Sci.*, 12, 97–106, doi:10.5194/nhess-12-97-2012, 2012.
- Little, T. A. and Rodgers, D. W.: 1855 Wairarapa Fault earthquake: world record strike-slip displacement now even bigger, in: *Programme and abstracts, Geoscience Society of New Zealand Miscellaneous Publications*, 117A, 64–65, 2004.
- Malamud, B. D., Turcotte, D. L., Guzzetti, F., and Reichenbach, P.: Landslides, earthquakes, and erosion, *Earth Planet. Sc. Lett.*, 229, 45–59, doi:10.1016/j.epsl.2004.10.018, 2004.
- McCahon, I., Mackenzie, J., Dewhurst, R., and Elms, D.: Grey District Lifelines study: Alpine fault earthquake scenario & lifelines vulnerability assessment, Grey District Council, 198 pp., 2005.
- McCahon, I., Dewhurst, R., and Elms, D.: West Coast Engineering Lifelines study: Alpine fault earthquake scenario, West Coast Regional Council, 204 pp., 2006a.
- McCahon, I., Dewhurst, R., and Elms, D.: Buller District Council Lifelines study: Alpine fault earthquake scenario, Buller District Council, 208 pp., 2006b.
- McSaveney, M. J.: The Sherman Glacier rock avalanche of 1964: its emplacement and subsequent effects on the glacier beneath it, Ph.D. thesis, Ohio State University, USA, 426 pp., 1975.
- McSaveney, M. J., Beetham, R. D., and Leonard, G. S.: The 18 May 2005 debris flow disaster at Matata: Causes and mitigation suggestions, *GNS Client Report*, 71, 51 pp., 2005.
- Miller, D.: The Alaska earthquake of July 10, 1958: Giant wave in Lituya Bay, *B. Seismol. Soc. Am.*, 50, 253–266, 1960.
- Nash, T., Bell, D., Davies, T. R. H., and Nathan, S.: Analysis of the formation and failure of Ram Creek landslide dam, South Island, New Zealand, *New Zeal. J. Geol. Geop.*, 51, 187–193, 2008.
- Nichol, S., Goff, J., Devoy, R., Chague-Goff, C., Hayward, B., and James, I.: Lagoon subsidence and tsunami on the West Coast of New Zealand, *Sediment. Geol.*, 200, 248–262, doi:10.1016/j.sedgeo.2007.01.019, 2007.
- Norris, R. J. and Cooper, A. F.: Late Quaternary slip rates and slip partitioning on the Alpine Fault, New Zealand, *J. Struct. Geol.*, 23, 507–520, doi:10.1016/S0191-8141(00)00122-X, 2001.
- Norris, R. J. and Cooper, A. F.: Origin of small-scale segmentation and transpressional thrusting along the Alpine fault, New Zealand, *Geol. Soc. Am. Bull.*, 107, 231–240, doi:10.1130/0016-7606(1995)107<0231, 1995.
- Ongley, M.: Surface trace of the 1855 earthquake, *Transactions of the Royal Society of New Zealand*, 73, 84–89, 1943.
- Parker, R. N., Densmore, A. L., Rosser, N. J., de Michele, M., Li, Y., Huang, R., Whadcoat, S., and Petley, D. N.: Mass wasting triggered by the 2008 Wenchuan earthquake is greater than orogenic growth, *Nat. Geosci.*, 4, 449–452, doi:10.1038/NGEO1154, 2011.
- Peterson, T., Ristau, J., Beavan, J., Denys, P., Denham, M., Field, B., François-Holden, C., McCaffrey, R., Palmer, N., Reyners, M., Samsonov, S., and The GeoNet Team: The Mw 6.7 George Sound earthquake of October 15, 2007: response and preliminary results, *Bulletin of the New Zealand Society for Earthquake Engineering*, 42, 129–141, 2009.

- Petrakov, D. A., Chernomorets, S. S., Evans, S. G., and Tutubalina, O. V.: Catastrophic glacial multi-phase mass movements: a special type of glacial hazard, *Advances in Geosciences*, 14, 211–218, 2008.
- Pettinga, J., Yetton, M., Van Dissen, R., and Downes, G.: Earthquake source identification and characterisation for the Canterbury region, South Island, New Zealand, *Bulletin of the New Zealand Society for Earthquake Engineering*, 34, 282–317, 2001.
- Pierson, T. C.: Erosion and deposition by debris flows at Mt Thomas, North Canterbury, New Zealand, *Earth Surf. Proc. Land.*, 5, 227–247, 1980.
- Power, W., Downes, G., McSaveney, M. J., and Beavan, J.: The Fiordland earthquake and tsunami, New Zealand, 21 August 2003, *Tsunamis*, 31–42, 2005.
- Quigley, M., Van Dissen, R., Villamor, P., Litchfield, N., Barrell, D., Furlong, K., Stahl, T., Duffy, B., Bilderback, E., Noble, D., Townsend, D., Begg, J., Jongens, R., Ries, W., Claridge, J., Klahn, A., Mackenzie, H., Smith, A., Hornblow, S., Nicol, R., Cox, S., Langridge, R., and Pedley, K.: Surface rupture of the Greendale Fault during the Mw 7.1 Darfield (Canterbury) earthquake, New Zealand: initial findings, *Bulletin of the New Zealand Society for Earthquake Engineering*, 43, 236–242, 2010.
- Reyners, M. and Webb, T.: Large earthquakes near Doubtful Sound, New Zealand 1989–1993, *New Zeal. J. Geol. Geop.*, 45, 109–120, 2002.
- Reyners, M., Gledhill, K., and Waters, D.: Tearing of the Subducted Australian Plate during the Te Anau, New Zealand, earthquake of 1988 June 3, *Geophys. J. Int.*, 104, 105–115, 1991.
- Reznichenko, N. V., Davies, T. R. H., and Alexander, D. J.: Effects of rock avalanches on glacier behaviour and moraine formation, *Geomorphology*, 132, 327–338, doi:10.1016/j.geomorph.2011.05.019, 2011.
- Rhoades, D. A. and Van Dissen, R.: Estimates of the time-varying hazard of rupture of the Alpine Fault, New Zealand, allowing for uncertainties, *New Zeal. J. Geol. Geop.*, 46, 479–488, 2003.
- Robinson, D. P., Brough, C., and Das, S.: The Mw 7.8, 2001 Kunlunshan earthquake: Extreme rupture speed variability and effect of fault geometry, *J. Geophys. Res.*, 111, B08303, doi:10.1029/2005JB004137, 2006.
- Robinson, R., Reyners, M., Webb, T., Arnadottir, T., Beavan, J., Cousins, J., Van Dissen, R., and Pearson, C.: The Mw 6.7 Arthur's Pass Earthquake in the Southern Alps, New Zealand, June 18, 1994, *Seismol. Res. Lett.*, 66, 11–14, 1995.
- Smith, W. D.: Spatial distribution of felt intensities for New Zealand earthquakes, *New Zeal. J. Geol. Geop.*, 21, 293–311, 1978.
- Smith, W. D. and Berryman, K.: Earthquake hazard in New Zealand: Inferences from seismology and geology, *Royal Society of New Zealand Bulletin*, 24, 223–243, 1986.
- Solov'ev, S. L. and Solov'eva, O. N.: Exponential distribution of the total number of an earthquakes aftershocks and the decrease of their mean value with increasing depth, *Bulletin of the Academic Sciences of the USSR Geophysics Series*, 1053–1060, 1962 (English Translation).
- Stauder, W.: The Alaska earthquake of July 10, 1958: seismic studies, *B. Seismol. Soc. Am.*, 50, 293–322, 1960.
- Sutherland, R.: Displacement since the Pliocene along the southern section of the Alpine Fault, New Zealand, *Geology*, 22, 327–330, 1994.
- Sutherland, R. and Norris, R. J.: Late Quaternary displacement rate, paleoseismicity, and geomorphic evolution of the Alpine Fault: Evidence from Hokuri Creek, South Westland, New Zealand, *New Zeal. J. Geol. Geop.*, 38, 419–430, 1995.
- Sutherland, R., Eberhart-Phillips, D., Harris, R. A., Stern, T., Beavan, J., Ellis, S., Henry, S., Cox, S., Norris, R. J., Berryman, K., Townend, J., Bannister, S., Pettinga, J., Leitner, B., Wallace, L., Little, T. A., Cooper, A. F., Yetton, M. D., and Stirling, M. W.: Do Great Earthquakes Occur on the Alpine Fault in Central South Island, New Zealand?, *Geoph. Monog. Series*, 175, 235–251, 2007.
- Tang, C., Zhu, J., Ding, J., Cui, X. F., Chen, L., and Zhang, J. S.: Catastrophic debris flows triggered by a 14 August 2010 rainfall at the epicenter of the Wenchuan earthquake, *Landslides*, 8, 485–497, doi:10.1007/s10346-011-0269-5, 2011.
- Tarr, R. S. and Martin, L. (Eds.): The earthquakes at Yakutat Bay, Alaska in September, 1899, *United States Geological Survey Professional Paper* 69, 1–131, 1912.
- Tocher, D.: The Alaska earthquake of July 10, 1958: Introduction, *B. Seismol. Soc. Am.*, 500, 217–322, 1960.
- USGS (United States Geological Survey): available at: <http://earthquake.usgs.gov/regional/nca/virtualtour/earthquake.php>, last access: 23 November 2012.
- Utsu, T.: Aftershocks and Earthquake statistics (1): some parameters which characterise an aftershock sequence and their interrelations, *Journal of the Faculty of Science, Hokkaido University, Series 7, Geophysics*, 3, 129–195, 1970.
- Utsu, T., Ogata, Y., and Matsu'ura, R. S.: The Centenary of the Omori Formula for a Decay Law of Aftershock Activity, *J. Phys. Earth*, 43, 1–33, 1995.
- Van Dissen, R. and Yeats, R. S.: Hope fault, Jordan thrust, and uplift of the Seaward Kaikoura Range, New Zealand, *Geology*, 19, 393–396, 1991.
- Wellman, H. W.: New Zealand Quaternary tectonics, *Geol. Rundsch.*, 43, 248–257, 1955.
- Wellman, H. W.: An uplift map for the South Island of New Zealand, and a model for uplift of the Southern Alps: Wellington, *Royal Society of New Zealand, Bulletin* 18, 13–20, 1979.
- Wellman, H. W. and Willett, R. W.: The Geology of the West Coast from Abut Head to Milford Sound – Part 1, *Transactions of the Royal Society of New Zealand*, 71, 282–306, 1942.
- Wells, A. and Goff, J.: Coastal dunes in Westland, New Zealand, provide a record of paleoseismic activity on the Alpine fault, *Geology*, 35, 731–734, 2007.
- Wells, A., Yetton, M. D., and Duncan, R. P.: Prehistoric dates of the most recent Alpine fault earthquakes, New Zealand, *Geology*, 27, 995–998, doi:10.1130/0091-7613(1999)027<0995, 1999.
- Whitehouse, I. E. and Griffiths, G. A.: Frequency and hazard of large rock avalanches in the central Southern Alps, New Zealand, *Geology*, 11, 331–334, 1983.
- Wood, H. O. and Neumann, F.: Modified Mercalli intensity of 1931, *B. Seismol. Soc. Am.*, 21, 277–283, 1931.
- Wright, C. A.: The AD 930 long-runout Round Top debris avalanche, Westland, New Zealand, *New Zeal. J. Geol. Geop.*, 41, 493–497, 1998.
- Xu, Q., Zhang, S., Li, W. L., and van Asch, Th. W. J.: The 13 August 2010 catastrophic debris flows after the 2008 Wenchuan earthquake, China, *Nat. Hazards Earth Syst. Sci.*, 12, 201–216, doi:10.5194/nhess-12-201-2012, 2012.

Yetton, M. D.: Progress in understanding the paleoseismicity of the central and northern Alpine Fault, Westland, New Zealand, *New Zeal. J. Geol. Geop.*, 41, 475–483, 1998.

Yetton, M. D., Wells, A., and Traylen, N. J.: The probabilities and consequences of the next Alpine fault earthquake, EQC, Research Report 95/193, available at: [http://www.eqc.govt.nz/research/researchpapers/p\\_019.aspx](http://www.eqc.govt.nz/research/researchpapers/p_019.aspx), last access: January 2013, 1998.